Università degli Studi di Ferrara

# DOCTORAL COURSE IN

" TRANSLATIONAL NEUROSCIENCE AND NEUROTECHNOLOGY"

CYCLE 37°

COORDINATOR Prof. Luciano Fadiga

*Mapping the neurophysiological Precuneus connectivity in Alzheimer's Disease patients from group to individual level: a TMS, EEG, and MRI integrated approach*

Scientific/Disciplinary Sector (SDS) BIO/09


**Candidate**

Dott. Esposito Romina

**Supervisor**

Prof. Koch Giacomo


Year 2021/2024

Content

1. Overview ..... 3
2. Brain Connectivity ..... 5
2.1. The brain network and its organization ..... 5
2.2. Connectivity measures ..... 7
3. Methods to study brain connectivity ..... 8
3.1. Structural and Functional MRI ..... 9
3.2. Diffusion MRI ..... 10
3.3. Electroencephalography (EEG) ..... 11
3.4. Transcranial Magnetic Stimulation (TMS) ..... 12
3.5. TMS-EEG integrative features ..... 13
3.6. TMS-EEG and MRI integrative features ..... 14
4. Mapping brain connectivity: network routing strategy ..... 18
5. Alzheimer's disease ..... 21
5.1. The Default Mode Network and the Relevance of the Precuneus ..... 22
6. Study: Mapping the neurophysiological Precuneus connectivity in Alzheimer's Disease patients from group to individual level: a TMS, EEG, and MRI integrated approach ..... 26
6.1. Abstract ..... 26
6.2. Introduction ..... 27
6.3. Materials and Methods ..... 28
6.3.1. Experimental design and participants ..... 28
6.3.2. MRI ..... 29
6.3.3. EEG ..... 30
6.3.4. TMS ..... 30
6.4. Data Pre-processing ..... 32
6.4.1. Structural and Functional MRI ..... 32
6.4.2. Selection of the first point of the Precuneus's grid ..... 32

6.4.3. Diffusion and Tractography ..... 33
6.4.4. Structural and Functional connectivity measures ..... 33
6.4.5. TMS-EEG ..... 35
6.5. Statistical Analysis ..... 36
6.6. Results ..... 38
6.6.1. TMS-EEG Recordings Comparison ..... 38
6.6.1.1 Sensor Space ..... 38
6.6.1.2 Source Space ..... 40
6.6.2. Nine-point grid signal propagation difference ..... 41
6.6.3. Subject-level characterization of source propagation ..... 44
6.6.4. TEPs and Source Correlations ..... 48
6.6.5. Source Activation and MRI Connectivity Measures Correlation ..... 52
6.7. Further proposed Investigations ..... 53
6.8. Implications and Insight ..... 55
6.9. Discussion ..... 57
6.10. Conclusion ..... 60
References ..... 61

# 1. Overview

Alzheimer's Disease (AD) consists of one of the neurodegenerative pathologies with a very high recurrence worldwide. Until today, several pieces of evidence have been accumulated to prove the need for a deeper comprehension of the neurophysiological characteristics. Even so, we must increase our knowledge of the activation and connectivity of the primary brain regions involved in AD neurodegeneration. In particular, at the individual level, we need to increase the possibility of recognizing the pathology at an early stage so that the treatment can obtain the maximum potential. In this study, I examined the activation and connectivity of one of the main regions involved in AD, the Precuneus, with an integrative and non-invasive approach. Firstly, I will provide general definitions of brain connectivity (Chapter 2). Considering all the connectivity measures, clearly defining such a complex concept is essential for describing the network organizations. Then, I will provide all the methods used until the present to explore brain connectivity (Chapter 3). "The majority of our knowledge of brain connectivity has been obtained from stand-alone neuroimaging methods" (Esposito et al., 2020). Nevertheless, choosing a methodologically integrative approach seems to bring great potential in investigating "effective brain connectivity, overcoming the limitations of single approaches" (Esposito et al., 2020). The proposed integrative TMS, EEG, and MRI represent a powerful tool for studying the neurophysiology features of the Precuneus, which is crucial in the connectivity alteration in AD patients and obtaining a reliable mapping of brain connectivity at the individual level (Chapter 4). Subsequently, a detailed description of Alzheimer's Disease and the interested brain region, the Precuneus, will be provided within the default mode network (Chapter 5). "The Default Mode Network is one of the neural networks active during the resting state, which is functionally connected with multiple cortical brain regions, forming the so-called *resting-state networks"* (Menon & Uddic, 2010). "This high functional connectivity within resting-state networks suggests the presence of direct structural connections between these functionally linked brain regions to facilitate ongoing interregional communication" (Menon & Uddic, 2010). Exploring the relationship between the white matter and the functional connections is crucial for shedding more light on resting-state connectivity.

Then, I will describe the experimental study that explored the activity and connectivity of the Precuneus with the proposed integrated approach (Chapter 6). For the first time, the TMS-EEG signal was recorded from a grid of nine points over the Precuneus, and it was possible to describe a map of activation at the individual level, thus reaching an informative

and reliable measure of brain connectivity. The obtained results suggest that, with the proposed integrated approach, it is feasible to map the Precuneus activity at both the group and subject levels, exploring the relationship between the functional and structural connectivity of the Precuneus in AD patients.

Lastly, the principal results and their relevance to the current knowledge of Precuneus connectivity in AD patients will be discussed, along with insight into the novel proposed integrated approach.

## 2. Brain Connectivity

### 2.1 The Brain Networks and its Organization

In recent years, the concept of a "network" has been mainly used to describe complex systems across many fields, including economics, politics, and biology. In the brain, this network concept has helped explain various neurobiological behaviors and theoretical concepts (Sporns, 2011). The intricacy of the brain is effectively represented by a network, emphasizing crucial aspects like organized connectivity patterns, multi-level structure, and nonlinear behavior. At a broader level, the brain's circuitry “forms a complex network comprising hundreds of areas and thousands of white matter” tracts that link these areas together (Sporns, 2011, 2013). These brain networks are organized in a hierarchical, nonlinear manner, and brain function results from the activation and reconfiguration of these dynamic networks. This ability to reorganize flexibly is essential for the brain to adapt to changing environments (Bassett & Sporns, 2017). Brain networks can be explored at various levels (Figure 1; Petersen & Sporns, 2015), from the level of individual cells (microscale) to that of entire brain regions (macroscale).

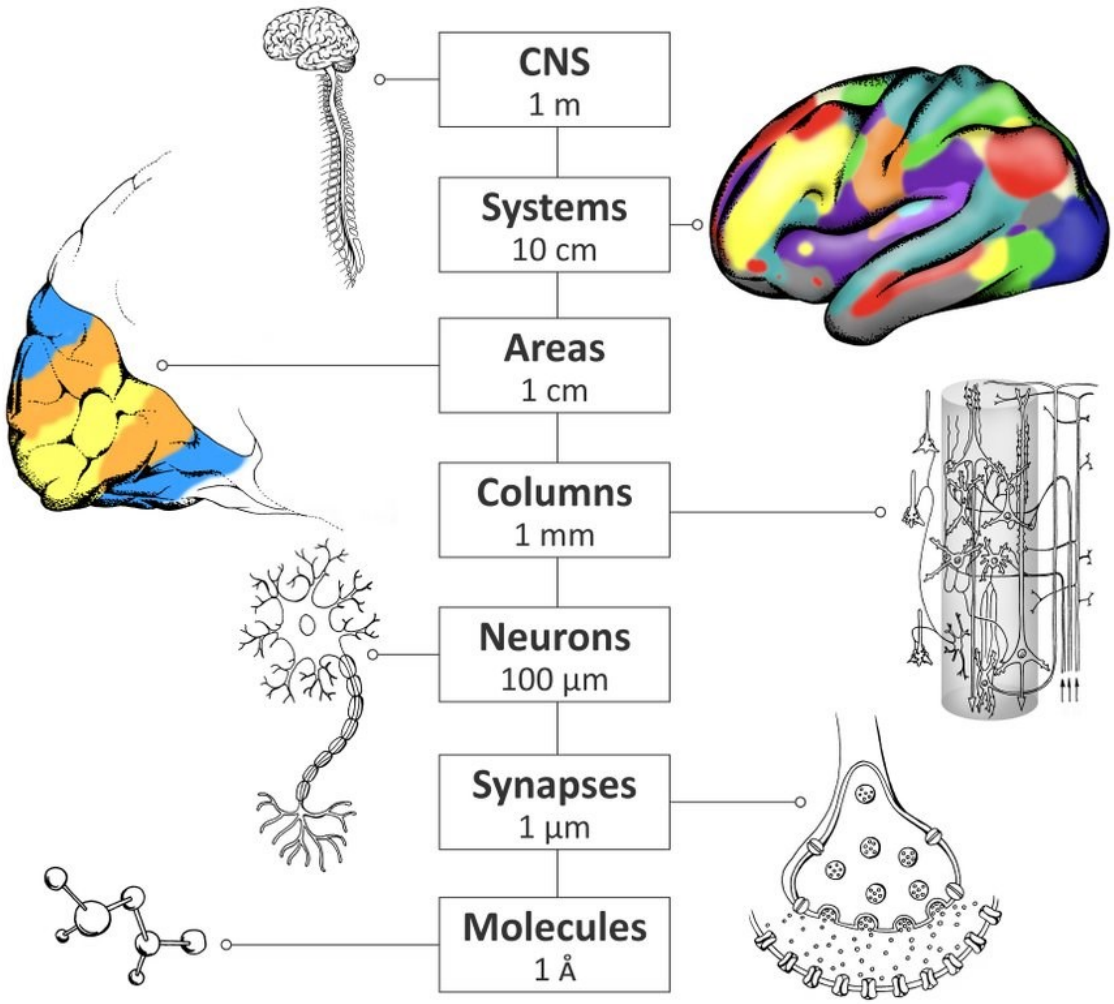


Figure 1 - Schematic representation of levels of structure within the nervous system.

Each level has its characteristics, and it is crucial to understand how each part works independently and in connection. The anatomical connections at all levels showed both specificity and variability. Specificity refers to how synaptic connections are arranged

between different types of neurons, how axons branch out, and how long-range connections are made between structures, such as brain regions or cell nuclei. Differences can be seen in the forms of individual neurons, the dimensions and locations of cerebral structures, and the connections between these structures. This variability exists not only between the brains of different individuals within the same species but also within the same person's brain over time, as the brain changes through growth, learning, and repair. This anatomical variability likely contributes to differences in brain function, neural activity, and behavior.

## 2.2 Connectivity Measure

Brain connectivity presents significant challenges because it is a multifaceted concept that cannot be reduced to a single unidirectional framework (Friston, 2011; Sporns & Betzel, 2016). When discussing brain connectivity, we refer to different types of connectivity: anatomical, functional, and effective connectivity, each offering unique insights into how distinct units within the nervous system interact (Figure 2).

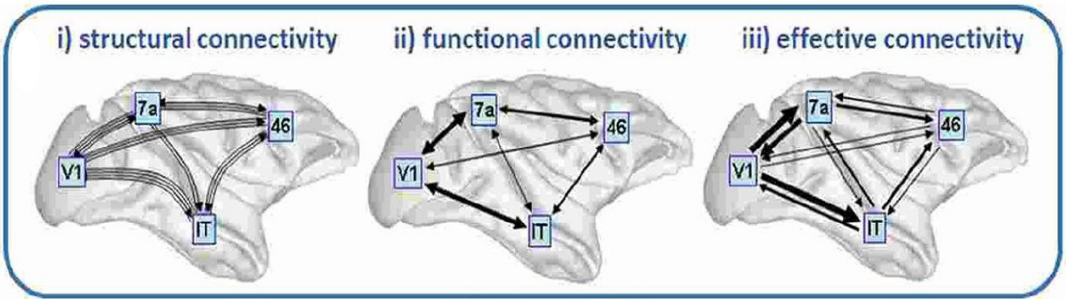


Figure 2 - Visualization of brain connectivity types. A) Diagrams depict three forms of neural connections in four regions of the macaque cortex: (i) structural connectivity, showing physical neural pathways; (ii) functional connectivity, indicating correlated activity; and (iii) effective connectivity, demonstrating the direction of information transfer. This illustration is based on Figure 1 from http://www.scholarpedia.org/article/Brain_connectivity and from Esposito et al.,2020.

Anatomical connectivity (Figure 2i) refers to physical or structural connections between neurons or groups of neurons, typically through synapses. These connections are characterized by parameters such as synaptic strength and efficacy. The physical arrangement of these anatomical links is relatively stable over short periods (seconds to minutes). However, significant changes can occur over extended periods (hours to days) due to plasticity and morphological adjustments. In contrast, functional connectivity (Figure 2ii) is a statistical concept. This reflects the statistical relationship between the spatially distant neuronal elements. Functional connectivity is commonly assessed using correlation, covariance, spectral coherence, or phase-locking measures. Importantly, functional connectivity does not require elements directly linked by structural connections and tends to vary over time. These statistical patterns can change rapidly, often within tens or hundreds of milliseconds, because the brain operates on multiple temporal scales. Functional connectivity does not indicate specific directional interactions or rely on any underlying

structural model. Effective connectivity (Figure 2iii) integrates anatomical and temporal information to determine "the causal influence of one neural system on another, either directly or indirectly" (Esposito et al.,2020). This connectivity provides insight into the causal dynamics between neural systems, offering a more detailed understanding of brain-network interactions.

## 3. Methods to Study Brain Connectivity

Contemporary research on brain connectivity has primarily utilized stand-alone neuroimaging techniques (Esposito et al., 2020). The main tools for investigation include "structural magnetic resonance imaging (MRI), functional MRI, diffusion tensor imaging, computational tractography, positron emission tomography, functional near-infrared spectroscopy, transcranial magnetic stimulation (TMS), electroencephalography (EEG), and magnetoencephalography" (Esposito et al., 2020). "Most of these neuroimaging methods focus on functional connectivity, whereas MRI and diffusion tensor imaging are used to examine anatomical connectivity" (Esposito et al., 2020) (Figure 3).

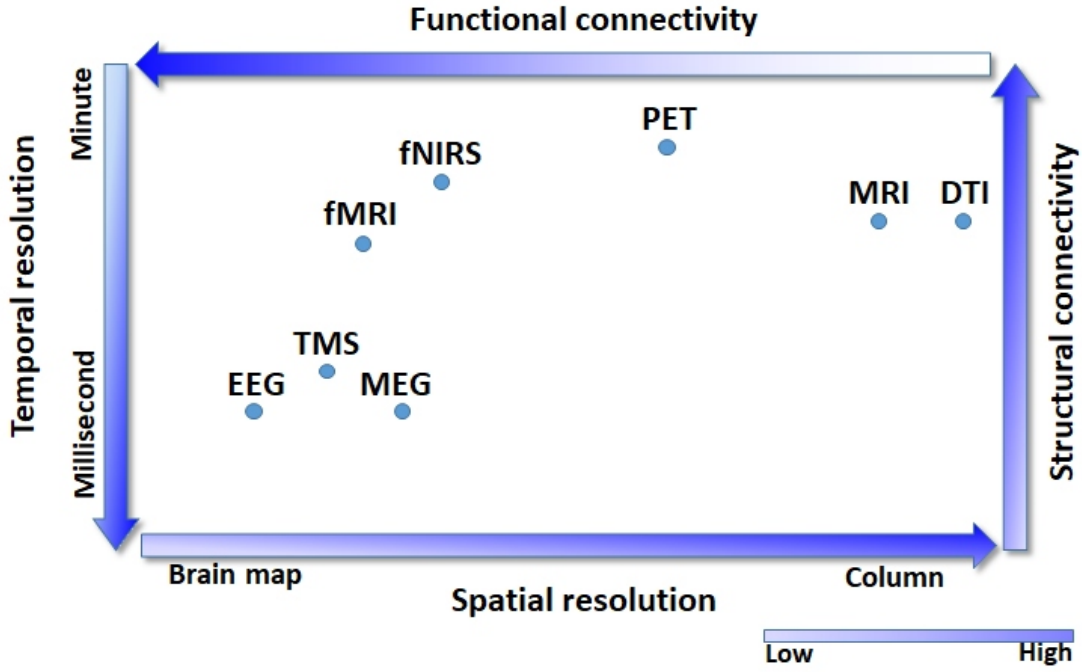


Figure 3 – "Connectivity can be represented based on a given method's resolution in this space. This figure shows the spatial and temporal resolution of the principal neuroimaging methods used to study brain connectivity. However, not just the spatial and temporal selectivity makes neuroimaging a useful experimental approach" (Esposito et al., 2020). Every "single method can also define functional or structural connectivity. An ideal

approach would integrate some of these techniques, covering a larger area of the figure space. fNIRS, functional near-infrared spectroscopy; PET, positron emission tomography; fMRI, functional magnetic resonance imaging; MRI, magnetic resonance imaging; DTI, diffusion tensor imaging; EEG, electroencephalography; TMS, transcranial magnetic stimulation; MEG, magnetoencephalography" (From Esposito et al., 2020).

Brain structures' form and function are interconnected through modular relationships (effective connectivity; see Friston and others, 1993; Sporns & Betzel, 2016) that adapt to environmental needs. Various factors influence active connections, including information type, processing requirements, subject state, past experiences, and the intricate interplay among these elements. Effective connectivity is challenging due to the neural system's constant bistability, where neurons fire or remain inactive based on system equilibrium. Consequently, understanding how dynamic neuronal patterns generate "human brain functions remains one of neuroscience's most fascinating and prevalent questions" (Esposito et al., 2020). We need to clearly understand how the complex structural brain architecture supports functional brain dynamics. We present "what we believe to be a promising approach to studying" brain connectivity (Esposito et al., 2020). This method integrates various techniques and mimics the nervous system's strategy of using individual element interactions to produce complex behavior. With the proposed study, when utilized in a comprehensive methodological context, TMS-EEG, guided by neuroimaging (tractography and MRI neuronavigation), became a promising tool for investigating the phenomenon's complexity, considering both a group-level exploration and an individual.

### 3.1 Structural and Functional MRI

In the last decades, structural and "functional magnetic resonance imaging has taken the lead in investigating brain organization and function" (Xu et al., 2016). The introduction of MRI in the late 1970s and early 1980s transformed neuroanatomy research, allowing for in vivo examination with sufficient contrast to distinguish brain regions (Lerch et al., 2017). Unlike the familiar analogy of "photographing the brain," "MRI detects radio-frequency signals emitted by hydrogen atoms after exposure to electromagnetic waves" (Lerch et al., 2017), using spatially varying magnetic gradients to pinpoint the signal. The contrast in each voxel (a three-dimensional pixel) is determined by proton density and local tissue microenvironment characteristics. These are directly linked to hydrogen's magnetic

properties or can be detected through magnetic field manipulation. The resulting contrast depends “on the specific timing of magnetic field manipulations, known as pulse sequences” (Lerch et al., 2017). While structural MRI focuses on examining brain anatomy and architecture, functional imaging is crucial for exploring short-term physiological changes associated with active brain function (Bandettini, 2012; Ugurbil, 2016). Functional neuroimaging seeks to associate different mental processes with specific brain regions, aiming to create a map of areas responsible for various cognitive functions. The activation maps obtained are derived from measuring blood oxygenation changes over time (Blood oxygenation level-dependent, BOLD). Blood oxygenation occurs naturally in normal brain physiology, with a temporal resolution of seconds.

### 3.2 Diffusion MRI

Diffusion magnetic resonance imaging (dMRI) measures the movement of water molecules in tissues. This movement, known as Brownian motion, occurs in three dimensions due to thermal collisions. In an isotropic environment, “water molecules diffuse uniformly in all directions, such as in a glass of water” (Killgore, 2021). Conversely, anisotropic diffusion occurs when water movement is directional and not random, like water flowing through straws. The more anisotropic the environment, the more linear and directional the water molecule diffusion becomes. In living organisms, water is distributed between cells and the extracellular matrix. Extracellular water typically moves more freely, while cell walls and other molecules constrain intracellular water. Consequently, water within cells follows paths determined by the structural arrangement of the walls. This results in high diffusion anisotropy in directional structures like white matter and muscle fibers. The human brain's white matter consists of axons that extend from neuronal cell bodies in gray matter to other brain regions or the spinal cord. These axons form bundles called white matter tracts, which are thought to connect functionally specialized but separate brain areas. Traditional MRI cannot visualize many of these tracts because it relies on T1 and T2 relaxation times, which are similar for white matter tracts regardless of their direction. Diffusion Tensor Imaging (DTI), corresponding to a variant of diffusion-weighted imaging, enables the visualization of white matter tracts by capturing the anisotropy of water diffusion (Figure 4). DTI achieves this by applying diffusion weighting in multiple spatial directions using diffusion-sensitizing gradients.

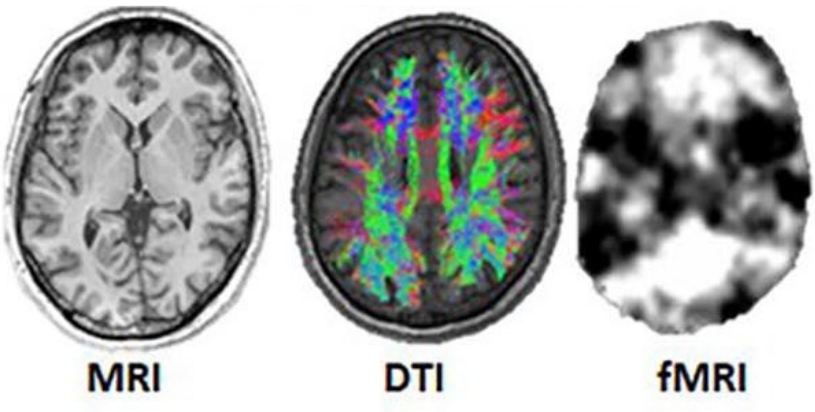


Figure 4 – The image shows how it looks like the same sagittal brain view within the different paradigms of image acquisition, from structural (MRI) to fiber reconstruction (DTI) to finally functional inspection (fMRI). (Adapted from Esposito et al., 2020).

The obtained data (Basser et al., 1994) “provides quantitative information about the brain's white matter in vivo”, at the voxel level, regarding the neuronal axons' local main direction(s). This data enables us to estimate the primary routes of extensive axon groups using polylines, referred to as streamlines. The complete collection of streamlines, known as a tractogram, represents the brain's structural connectivity network (Sporns et al., 2005). Tractography is the medical imaging operation that reconstructs 3D fibers starting from diffusion data and proprieties. Locating the pathway of fiber systems enables delineating the connectivity of an anatomical region with a certain level of confidence before being exclusive to invasive methods. Tractography can offer an improved way to provide an in vivo definition of brain anatomy.

### 3.3 Electroencephalography (EEG)

H. Berger conducted the initial electroencephalography (EEG) in the 1920s, documenting brain alpha waves for the first time. Despite early doubts, this technique gained widespread acceptance in clinical and research settings. EEG captures the electrical activity produced by groups of neurons positioned perpendicular to the scalp. The detected

signal traverses multiple layers of neural tissue, blood, CSF, meninges, skull, and skin. The EEG signal is believed to represent the spatial and temporal sum of excitatory and inhibitory postsynaptic potentials (EPSP or IPSP) within a neuronal cluster. The EEG system requires at least two electrodes - a recording sensor and a reference - to measure potential differences between two areas. These electrodes connect to an amplifier and an analog-to-digital converter for signal digitization. Generally, this method is employed in two primary ways: continuous recording without a specific time-linked event or event-related recordings associated with processing internal or external stimuli (Luck, 2014).

## 3.4 Transcranial Magnetic Stimulation (TMS)

The operational mechanism of transcranial magnetic stimulation (TMS) is rooted in the electromagnetic induction principle, as elucidated by Faraday's law. The technique employs a rapid, powerful electric current flowing through a wire coil. This current generates a magnetic field reaching 3 T, lasting approximately 100 μs. When positioned on the scalp, this magnetic pulse penetrates the skull unimpeded, creating a secondary electric field within brain tissue. This TMS-induced current can directly cause neuronal depolarization or alter neural excitability (Kobayashi & Pascual-Leone, 2003). The initial TMS device sanctioned for clinical use was developed by A. Barker in 1985 (Barker, Jalinous, & Freeston, 1985). When utilized by established guidelines (Rossi et al., 2011; Rossini et al., 2015), TMS enables non-invasive interference with neuronal activity. The impact of TMS on neural structures was primarily examined by stimulating the motor cortex and measuring the resulting muscle action potential in a peripheral target muscle (known as motor-evoked potentials, MEP) (Nakamura et al., 1996; Di Lazzaro et al., 1998, 1999). These studies, involving epidural recordings from patients with cervical electrode implants, revealed that TMS can produce bursts of descending direct waves (D-waves) and indirect waves (I-waves). Researchers hypothesized that D-waves result from the direct activation of pyramidal neurons, while I-waves stem from the indirect activation of pyramidal neurons through interneuron depolarization (Day et al., 1987). The effects observed in these studies are believed to occur similarly when TMS targets non-motor brain regions.

### 3.5 TMS-EEG integrative features

Over the past 20 years, researchers have identified TMS-EEG as an optimal method for examining cortical responsiveness and functional connectivity in both healthy individuals (Rogasch & Fitzgerald, 2013; Siebner and others, 2009; Thut & Pascual-Leone, 2010) and those with pathological conditions (e.g., Ragazzoni and others, 2017). Scientists can explore communication within and across neural networks by integrating single-pulse TMS with EEG. This is achieved by utilizing "EEG to monitor the activity triggered by TMS, which spreads, either directly or indirectly, to anatomically and functionally linked regions (Bonato et al., 2006; Ilmoniemi and others, 1997; Rogasch et al., 2013; Voineskos and others, 2010)" (Esposito et al., 2020). The combination of EEG and TMS offers a robust technique for measuring brain activity and investigating causal relationships between brain areas during cognitive task performance and brain functions (Bortoletto and others, 2015). Research has shown that cortical responses recorded using TMS-EEG demonstrate high reproducibility across various cortical areas and are sensitive to changes over time (Casarotto and others, 2010; Farzan and others, 2010; Kerwin et al., 2018; Lioumis et al., 2009). For example, Casarotto and others (2010) conducted a single-subject comparison to assess "the similarities and differences between pairs of TEPs recorded under identical or different stimulation conditions" (Esposito et al., 2020). The resulting measure (Divergence Index, DI) successfully detected "whether a change in perturbation parameters had occurred, thus demonstrating that" TEPs are responsive to longitudinal changes (Esposito et al., 2020). TMS-induced neural activity can be assessed with high spatio-temporal precision by examining the resulting physiological responses, known as TMS-evoked potentials (TEPs; Hill et al., 2016, but see Conde and others 2019). These complex waveforms, synchronized with the TMS pulse, exhibit peaks and troughs at various latencies. While TEPs are primarily measured from the motor cortex, they can also be observed in other cortical regions (Bagattini et al., 2019; Rosanova et al., 2009). The activation spreads to connected areas, both nearby and distant (Komssi and others, 2002), following intra- and interhemispheric association fibers. The interaction between the induced electric field and neural tissue influences the extent of cortical activation. A more substantial TMS effect corresponds to a stronger induced electric field. The intensity of the TMS effect is determined by coil and "stimulation parameters, such as coil position and orientation, which impact neuronal excitation" (Esposito et al., 2020). It should be noted that TMS-EEG may also stimulate the peripheral nervous system, necessitating appropriate control conditions in connectivity protocols (Conde and others, 2019). Connectivity can be evaluated by examining TEP

amplitudes and latencies across the scalp. An alternative method involves computing the area under the TEP curve (Pellicciari et al., 2013), representing TMS's impact on brain activity at specific or across all electrodes (mean field power). Additionally, TMS-EEG allows for exploring TMS effects in the frequency domain, enabling the investigation of the "functional specificity of brain rhythms in cognition" (Thut & Miniussi, 2009; Esposito et al., 2020). TMS-evoked oscillations "can be assessed as an evoked oscillatory response, providing information on oscillations phase-locked to the TMS pulse, or as a total oscillatory response (also called event-related spectral perturbation)" (Esposito et al., 2020). This approach captures phase- and non-phase-locked oscillations following TMS (Pellicciari et al., 2017). TMS-EEG measurements are valuable tools for identifying potential biomarkers in various neurological (Koch et al., 2019) and psychiatric conditions. Research by Koch and colleagues 2018 demonstrated the utility of TMS-EEG measurements in assessing AD patients before and after treatment protocols. The TMS-EEG signal indicated heightened neural activity in the parietal cortex (quantified using Global Mean Field Power, GMFP) and enhanced beta band brain oscillations. Additionally, it enabled the evaluation of "changes in functional connections between the parietal cortex and medial frontal regions within the Default Mode Network" (Esposito et al., 2020). "A recent review (Hui et al., 2019) highlighted evidence suggesting that alterations in gamma oscillations in prefrontal areas are associated with depression and that TMS-EEG could potentially identify this as a reliable biomarker. Further studies (Colombo et al., 2019) have explored the possibility of deriving indices from TMS-EEG to aid in diagnosing and assessing clinical conditions, such as consciousness disorders" (Esposito et al., 2020).

### 3.6 TMS, EEG, and MRI integrative features

Most of our understanding of brain connectivity stems from individual neuroimaging techniques, each with advantages and limitations. To overcome these constraints, researchers combine different methods to enhance the quality and scope of information gathered.

EEG is a non-invasive technique that effectively studies the brain's electrophysiological dynamics and their relationship to cognition and disease (Buzsáki & Draguhn, 2004; Cohen, 2017). A significant challenge in neuroscience has been to shed more light on the neural basis of effective connectivity by integrating EEG with other methods like TMS and MRI.

Precisely examining temporal patterns through EEG can inform the timing of TMS stimulation. By synchronizing TMS with EEG-derived temporal information, researchers can reduce inter and intra-individual variability in TMS interactions, increasing its effectiveness (Thut and others, 2017; Ziemann & Siebner, 2015). Given these developments, future research will likely use real-time EEG-derived temporal dynamic information to guide TMS application.

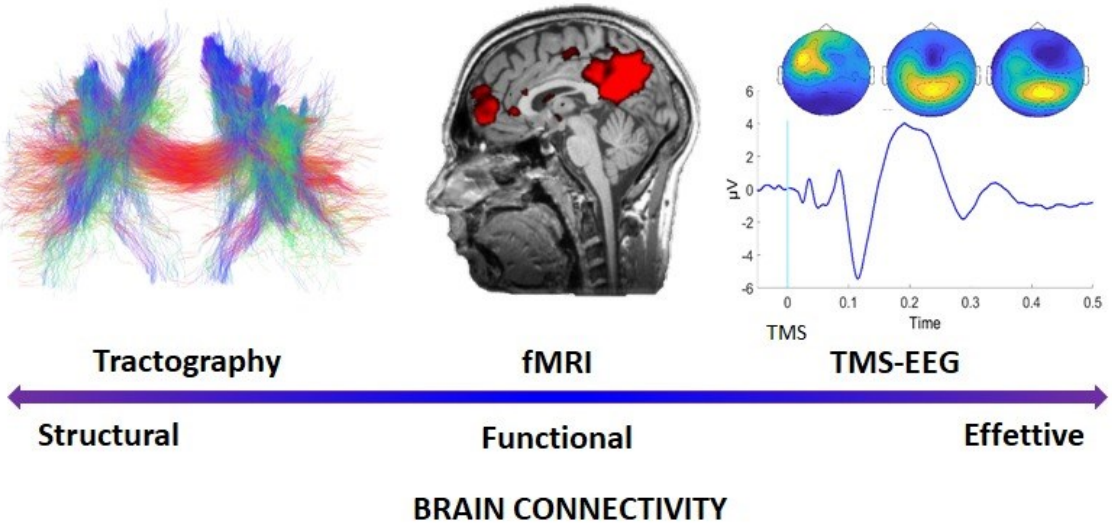


Figure 5 - Three neuroimaging techniques (DTI tractography, fMRI, and TMS-EEG co-registration) and the specific type of brain connectivity each method can measure: "structural, functional, and effective, respectively. Integrating these neuroimaging approaches enables a more comprehensive understanding of cortical connectivity" (Esposito et al., 2020). Primarily when implemented during peak information exchange between brain regions (Picture from Esposito et al., 2020).

Despite its advantages, TMS-EEG faces limitations in spatial resolution (Figure 5). Researchers need help measuring neural activity below the cortex and accurately identifying signal sources. To overcome these challenges, MRI data can be integrated with TMS-EEG, potentially achieving a higher level of integration than EEG alone through multimodal brain imaging fusion. MRI provides a more precise spatial definition of regions of interest, offering accurate constraints for TMS navigation (Ning et al., 2019). Ning and colleagues (2019) demonstrated a quantitative assessment of topographic precision and variability in identifying cortical targets for neuromodulation. They highlighted how data quality and pre-processing factors can affect targeting reliability. Various factors influence TMS spatial

resolution, including coil orientation, pulse intensity, and head/brain anatomy" (Esposito et al., 2020). While the stimulated cortical area can vary based on TMS parameters, it should be smaller than the topographical variability observed in MRI-based targeting strategies. This suggests that MRI targeting strategies may have more significant topographical variability than TMS's spatial resolution, potentially resulting in missed stimulation of the intended target. Although the literature has identified average areas involved in cognitive tasks, individual brain structure and function differences exist. Using precise MRI-derived target coordinates allows for a more accurate definition of structural nodes, leading to a more precise TMS-EEG connectivity evaluation with spatial constraints. Additionally, correlation analysis may help assess the impact of individual spatial patterns on connectivity (Figure 6), as different brain architectures may lead to variations in functional signal propagation. Combining TMS-EEG and MRI data could enhance structural resolution and enable millimeter-precise stimulation of relevant nodes. However, this technical advancement may not necessarily translate to improved cognitive and functional resolution, potentially only increasing spatial constraints without significant benefits. To reach a more profound understanding of the relationship between structurally connected areas and their functions, we should utilize the latest advancements in neuroimaging technology. Analysis of the brain's intricate structural organization and the insights provided by diffusion imaging offer quantitative data about the brain's white matter. Through the application of mathematical models known as "constrained spherical deconvolution (Tournier et al., 2007), it becomes possible to estimate fiber orientation distributions and generate tractograms (Olivetti et al., 2016; Porro-Muñoz and others, 2015). These tractograms represent the brain's structural connectome and can serve as" a foundation for planning specific investigations of effective connectivity (Esposito et al., 2020). By examining the graph's dimension, node depth, and tractogram quantity, we can assess how these parameters relate to the network's functionality. "The high spatial resolution offered by MRI and tractograms can enhance our understanding of brain architecture" (Bullmore & Sporns, 2009; Esposito et al., 2020). A map of brain architecture can be constructed by connecting each local neuronal community. This implies that all nodes in an extensive system are connected through "relatively few intermediate steps. However, most nodes maintain only a limited number of direct connections within a neighboring clique" (Borgatti et al., 2009; Esposito et al., 2020). "The resulting architectural map illustrates the structural connection pattern of each node with others. This aligns with combining structural (Stephan et al., 2009) and functional connectivity to provide constraints that inform effective connectivity (Seghier & Friston, 2013). The functionality of these nodes may vary based on their interactions and can be

evaluated using TMS-EEG. Consequently, different functional organization rearrangements may correspond to different measurements. Therefore, the proposed TMS-EEG MRI integrative approach" will enable the provision of robust and informed structural constraints for exploring neurophysiological signal propagation within the complex brain architecture (Esposito et al., 2020). Simultaneously, it will allow for studying signal flow prediction among the fibers delineated by tractography. Recent studies have employed graph theory to examine "the topological organization of brain properties regarding regional connectivity (Bassett & Sporns, 2017; Bassett & Bullmore, 2006). Graph theory has" contributed to elucidating the connection between human cognitive functions and neuronal network structures by applying models called graphs, which describe brain connectivity (Esposito et al., 2020). "The TMS-EEG MRI approach generates directed graphs. In this context, nodes are detectable through functional MRI, edges are measurable via diffusion imaging, and directions are tested using TMS-EEG" (Esposito et al., 2020).

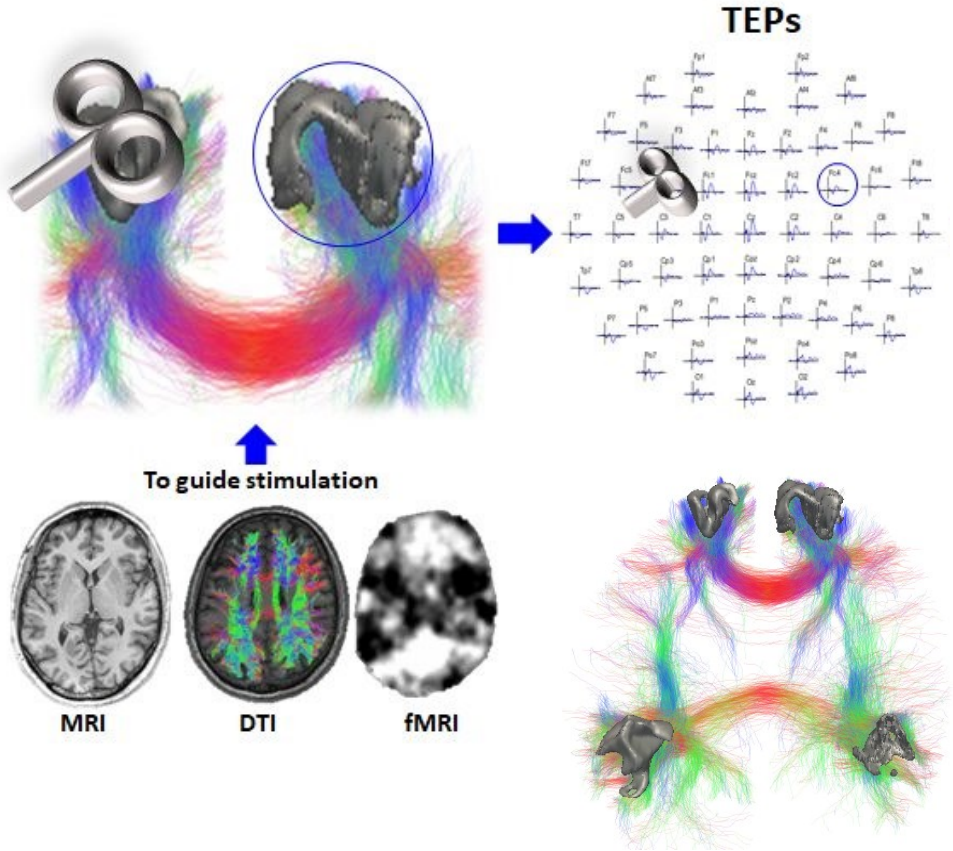

Figure 6 - The illustration depicts the potential for combining TMS-EEG and DTI through correlation analysis. a) Two cortical regions (depicted in grey) are shown to have a direct structural connection. In this example, “single-pulse TMS is applied to the left region of interest (ROI). b) TMS-evoked potentials (TEPs) are recorded in the area opposite the stimulated region, which is structurally” linked (indicated by a blue circle) (Esposito et al., 2020). These TEPs are averaged, and each time point is correlated with the tractogram's size. In the TEP graph, significant components are highlighted with grey bars. Below the graph, topographic correlations are displayed, supporting the structural connectivity findings. (Adapted from Esposito et al., 2022)

## 4. Mapping brain connectivity: network routing strategy

One of today's most significant scientific challenges is understanding the brain's structure and function. As mentioned earlier, the integrative approach shows promise in achieving this goal. By combining TMS-EEG and MRI techniques, researchers can gain a comprehensive view of brain function at the macroscopic level, encompassing spatial (structural pathways via MRI), temporal (cortical activity timing through EEG), and effective (directional information from TMS) aspects (Figure 7). This method enhances our ability to examine the causal connections between brain architecture and dynamics, potentially revolutionizing our comprehension “of brain connectivity (Avena-Koenigsberger et al., 2017). The integrative approach” (Esposito et al., 2020) could also improve our understanding of signal communication within complex neural networks. By determining the spatio-temporal routes signals use under various circumstances, we can gain deeper insights into how information spreads throughout the brain. “These information pathways may vary (Avena-Koenigsberger and others, 2019), with some EEG signal components traveling along short, direct routes while others take more intricate paths through multiple nodes within the same networks” (Esposito et al., 2020). Recently, there has been growing enthusiasm for utilizing network models (network neuroscience) to elucidate and forecast system functionality. The structural arrangement of connections can influence the interaction patterns among system components, which governs overall system behavior. Communication routing refers to the ability of two network nodes to interact when connected by a pathway, with the pathway's length playing a crucial role in communication effectiveness. In biological neural systems, for instance, “the number of synapses between systems is ideally” kept to a minimum,

considering that longer pathways increase the risk of noise and metabolic expenses (Esposito et al., 2020).

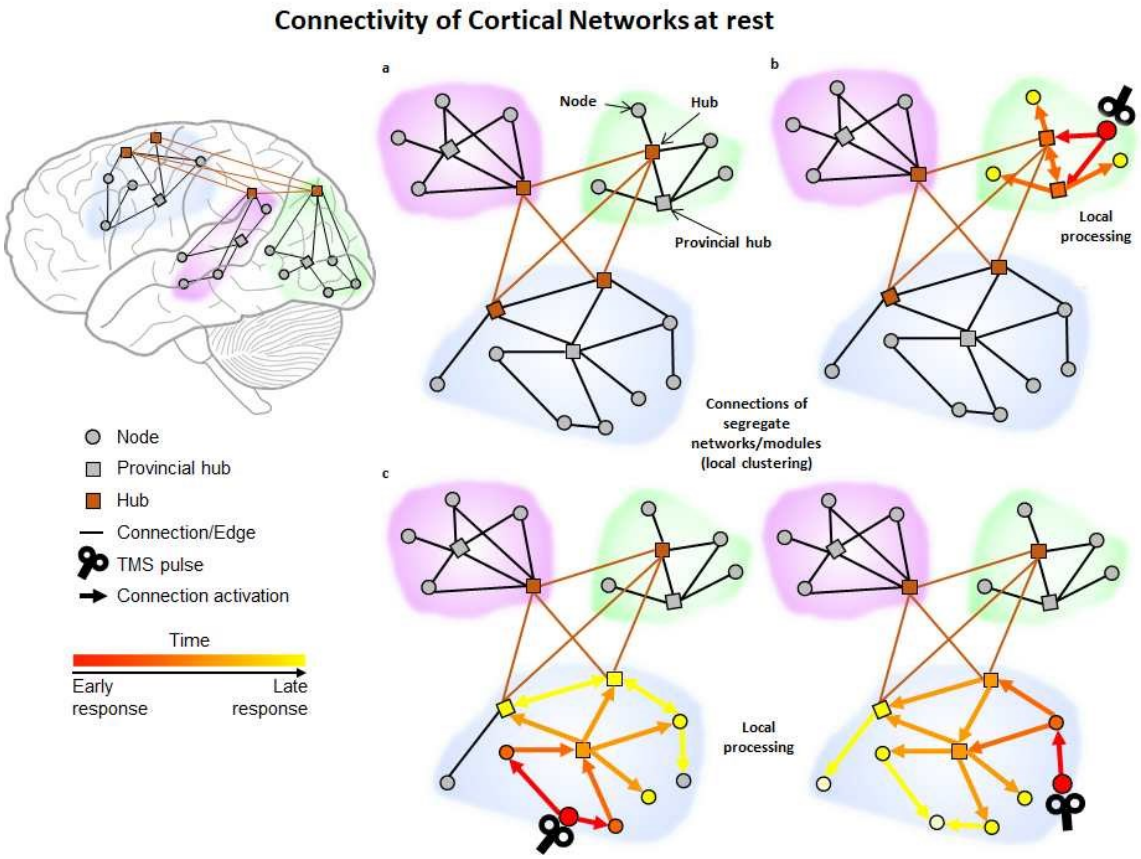


Figura 7 - Incorporating physiological data from TMS-EEG could enhance network modeling, leading to a more accurate depiction of signal transmission within network components. The figure (from Bortoletto and others, 2015) illustrates the brain network's modular structure. (a) It displays “nodes (grey circles), local hubs (grey squares), and rich-club hubs (red squares), along with their short-range (black lines) and long-range (red lines) connections. (b) Colored arrows indicate the causal interactions between nodes and the timing of signal propagation following the TMS pulse. Post-TMS, the stimulated area's activation spreads to other nodes within the same module via short-range connections. (c) When TMS stimulates two lower-degree nodes in the same network, the signal travels within that module. Initially, different nodes are activated (site-specific responses), followed by the eventual activation of hubs connected to both initial sites (site-invariant responses)” (Esposito et al., 2020).

While routing communication effectively describes small network interactions, it becomes more complex when dealing with larger, more intricate systems. Modeling information

processing in extensive networks poses significant challenges (Tadić et al., 2019). The complexity of explaining brain information flow stems from "the nature of electrophysiological signals (Deslauriers-Gauthier and others, 2019; Rossini and others, 2019) (Esposito et al., 2020). Various signal components may encode distinct information, potentially following multiple pathways. Consequently, "the overall information flow is distributed across all routes of each signal component" (Esposito et al., 2020). Understanding "the functional dynamics is crucial for" elucidating how information efficiently traverses different network elements through complex topologies (Deriche, 2016; Esposito et al., 2020). Leveraging the advantages of "integrated TMS-EEG and MRI techniques can help elucidate the physiological basis of this information flow" (Esposito et al., 2020). Researchers can better understand the relationship between network dynamics and topology by "correlating spatially distributed physiological signals with structural pathways" (Esposito et al., 2020). Moreover, this approach may have positive implications in clinical settings. The proposed integrated method could serve as a valuable tool for quantifying previously subjective signal signatures with increased sensitivity.

## 5. Alzheimer’s Disease

Alzheimer’s disease corresponds as the principal cause of dementia worldwide (Mayeux & Stern, 2012). This neurological condition predominantly impacts elderly individuals. This disorder is characterized by steadily deteriorating cognitive functions, such as memory and linguistic abilities, reasoning, and executive functions, which increasingly impair an individual’s ability to perform everyday activities and maintain individual independence. With no known cure, Alzheimer’s poses a growing public health challenge as populations age, affecting not only patients but also their caregivers and healthcare systems globally. “Alzheimer's disease is characterized by abnormal buildups of two protein types in the brain: amyloid-beta and tau” (Nekkalapu 2024). The first is amyloid plaques, composed of adhesive aggregates of beta-amyloid fragments, which mainly interfere with neuronal communication. Instead, the tau proteins typically help maintain neuronal structure, become impaired, and create neurofibrillary tangles inside brain cells, disrupting their internal transport mechanisms. All these pathological changes lead to the death of neurons and progressive brain atrophy. The main impaired brain regions are the hippocampus and frontal lobes, which are crucial for memory, learning, and decision-making. The disease progresses in stages. In its early phase, patients may experience mild forgetfulness and difficulty concentrating, often mistaken for typical signs of aging. As Alzheimer’s advances to the moderate stage, memory loss worsens, confusion sets in, and individuals may struggle to recognize familiar people or places. In the later stages, patients become entirely dependent on caregivers due to the loss of physical coordination, speech, and cognitive abilities. We do not know precisely the cause of Alzheimer’s disease yet. However, it is believed to result from a complex genetic, environmental, and lifestyle interaction. Genetic predisposition plays a role, with specific gene mutations like APOE ε4increasing the risk. However, not everyone with these genes develops Alzheimer’s. The environment and lifestyle factors may also influence disease onset. Moreover, head injuries, cardiovascular conditions, and chronic diseases such as diabetes have been identified as contributing risk factors. However, age remains the most significant risk factor for Alzheimer’s disease. “The burden of Alzheimer’s disease on individuals, families, and healthcare systems” is immense (Nekkalapu, 2024). The disease not only affects cognitive abilities but also places emotional, physical, and financial stress on caregivers, often family members, who provide essential care and support throughout the disease's progression. The diagnosis of neurodegenerative pathology of Alzheimer's is primarily done through a combination of clinical evaluations, cognitive tests, and brain imaging techniques. Recently, researchers have increasingly focused on

identifying biomarkers, such as specific proteins in cerebrospinal fluid or beta-amyloid levels in blood, to detect the disease in its earliest stages, even before symptoms appear. While there is currently no cure for Alzheimer's, modern treatments aim to preserve symptoms and slow the progression of cognitive decline. Medications like cholinesterase inhibitors and NMDA receptor antagonists help enhance communication between neurons and temporarily improve cognitive functions. In recent years, innovative therapies targeting amyloid plaques have shown promising results in clinical trials. The hope for future breakthroughs in treatment and life condition improvement is highly supported.

## 5.1 The Default Mode Network and the Relevance of the Precuneus

Among the initial indicators of typical Alzheimer's disease (AD), memory deterioration stands out as a primary symptom, and currently, no effective treatments exist. Recent research has highlighted the precuneus (PC) as a crucial region associated with the memory deficits observed in early-stage AD. This importance is likely attributed to disruptions in connectivity within extensive neural networks, particularly the default mode network (DMN).

In 1997, researchers first observed a group of regions "in the human cerebral cortex that consistently showed reduced activity during various novel goal-oriented tasks" (Shulman et al., 1997). These activity decreases were consistently present across different tasks. The next "challenge was to demonstrate that these reductions were not caused by activations in the resting state due to uncontrolled" cognitive processes (Raichle, 2015). A significant PET study (M E Raichle et al., 2001) revealed "that the brain areas exhibiting decreased activity during attention-demanding goal-directed tasks were not activated in the resting state". Instead, these decreases indicated a previously "unrecognized organization within the brain's intrinsic or ongoing activity" (Raichle, 2015). Later, additional brain regions were found to be part of this network involved in intrinsic brain activity. This discovery sparked interest in studying "the brain's resting state. The default mode network (DMN)" (Marcus E Raichle, 2015) consists of three main components: "the ventral medial prefrontal cortex, the dorsal medial prefrontal cortex, and the posterior cingulate cortex", which includes the neighboring precuneus and lateral parietal areas (approximately Brodmann area 39) (Figure 8). Additionally, the entorhinal cortex is often linked to the DMN. The ventral medial prefrontal cortex (VMPC) plays a crucial role in a network of regions (Ongur & Price, 2000; Price,

2007). It receives sensory input “from the external environment and the body through the orbital frontal cortex” (Raichle 2015). It transmits this “information to structures like the hypothalamus, amygdala, and midbrain's periaqueductal gray matter” (Raichle 2015). This anatomical arrangement suggests that the VMPC component of the DMN functions “as a sensory-visceromotor connection involved in social behavior, mood regulation, and motivational drive, which are fundamental aspects of an individual's personality” (Raichle 2015).

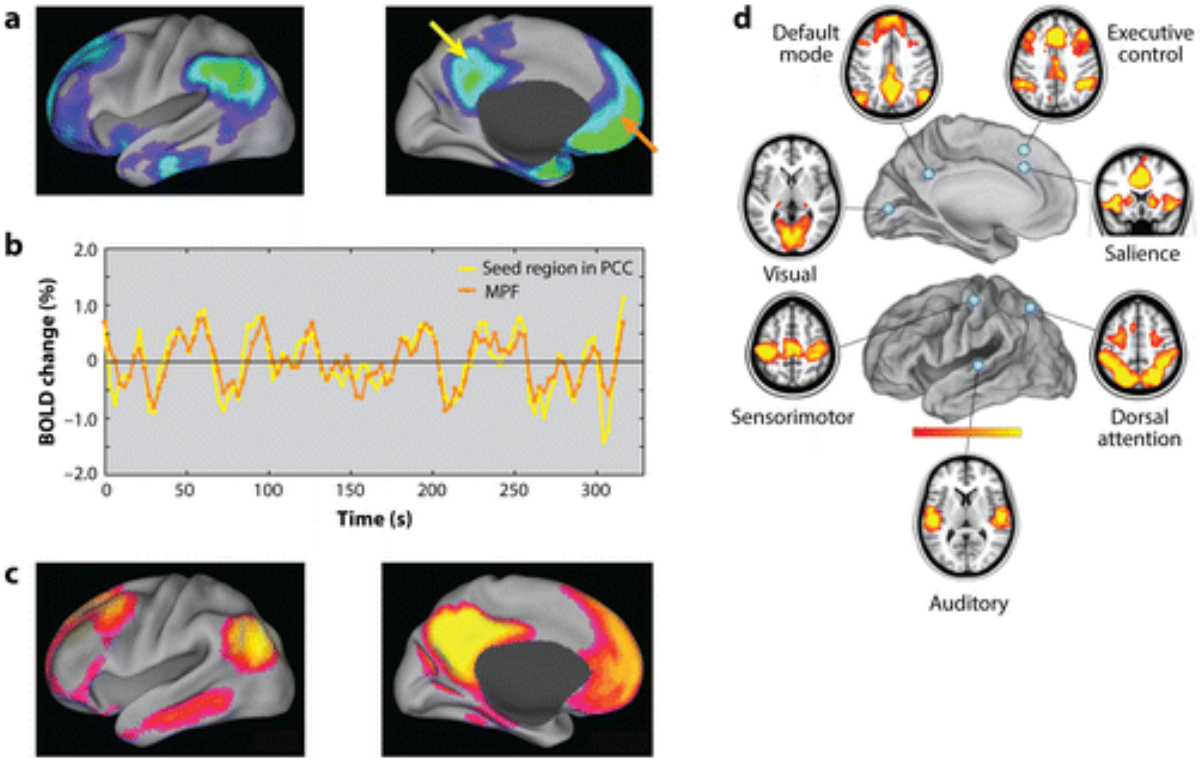


Figura 8 - The default mode network is examined from multiple angles: its reduced activity during task execution (illustrated in panels b and c), its functional connectivity during rest, and its relationship to other networks exhibiting resting-state functional connectivity patterns (shown in panel d). In panel a, yellow and orange arrows indicate the origin of the blood-oxygen-level-dependent “(BOLD) resting-state time-activity curves displayed in panel b” (Raichle 2015). “The medial prefrontal cortex (MPF) and the precuneus and posterior cingulate cortex (PCC)” are key areas highlighted (Menon & Uddic 2010). This figure incorporates elements adapted from Raichle (2010, 2011, 2015).

The VMPC component of the DMN represents “a dynamic equilibrium between focused attention and emotional state, potentially arising from a functionally active baseline”

(Raichle, 2015). The neighboring “dorsal medial prefrontal cortex (DMPC) is distinguished from the VMPC by its association with self-referential judgments” (Seitz et al., 2009). Increased DMPC activity is typically accompanied by decreased VMPC activity, aligning “with the observation that attention-demanding tasks diminish emotional processing” (Raichle, 2015). Other significant elements of the DMN incorporate the posterior cingulate cortex and the medial precuneus. Functional connectivity evidence has revealed a “strong relationship between hippocampal formation and the posterior components of the DMN” (Umeda, 2018). “This hippocampal-parietal memory network exhibits notable daily fluctuations, being active in the evening and inactive in the morning following a typical night's sleep. This finding indicates that the connection between the hippocampal formation and the posterior DMN” components is influenced by cumulative waking experiences and is reset daily by sleep (Raichle, 2015). In conclusion, Buckner, Andrews-Hanna, and Schacter (2008) suggest that the function of this continuous and intrinsic brain activity is likely related to processes supporting “emotional processing (VMPC), self-referential mental activity (DMPC), and recollection of past experiences (posterior DMN components)” (Raichle, 2015). Regardless of cognitive tasks, the DMN remains active, modulating its activity by decreasing or increasing it. “The default mode network (DMN) is a group of interconnected brain regions that show increased activity during periods of mental rest and decreased activity when engaged in externally focused tasks (Marcus E Raichle, 2015). DMN activity is linked to internal cognitive processes (Buckner et al., 2008) and can be impacted by various neurological disorders (Castellanos et al., 2013). Consequently, researchers are investigating the DMN and its alterations to establish it as a dependable, non-invasive biomarker (Marchitelli et al., 2016). Several neurological and psychiatric conditions are associated with disruptions in the DMN's structural and functional connectivity. For example, extensive research has been conducted on the relationship between DMN and Alzheimer's disease (AD) (Dillen et al., 2017; Koch et al., 2018). AD typically manifests as impairments in acquiring new information and recalling existing memories. This decline in long-term episodic memory is attributed to localized damage in the medial temporal lobes and dysfunction of extensive networks involved in “memory processes. From the early stages of AD, significant neuropathological alterations (such as β-amyloid plaques and neurofibrillary tangles) are known to affect posterior cortical regions, including the precuneus, posterior cingulate, retrosplenial, and lateral posterior parietal cortex (Buckner et al., 2005). These abnormalities are accompanied by an initial disruption of medial frontoparietal functional connectivity, as evidenced by alterations in the DMN, of which the precuneus is a crucial component” (Buckner et al., 2008; Marcus E Raichle, 2015). The

disconnection of the precuneus occurs before and likely contributes to regional brain atrophy, which becomes more pronounced in the later stages of the disease (Gili et al., 2011). As a result, the precuneus is considered a vulnerable area during the transition to dementia. It may serve as an ideal target for specialized interventions to mitigate AD-related memory decline. “Alzheimer's disease (AD) typically manifests with deficits in learning new information as well as in retrieving old memories (Bäckman et al., 2001). This impairment in long-term episodic memory has been attributed to local damage of the medial temporal lobes and dysfunction of large-scale networks underlying memory processes”. From “the early stages (see above) of AD, significant neuropathological abnormalities (i.e., β-amyloid plaques and neurofibrillary tangles) are known to affect the posterior cortical regions of the brain, including the precuneus (PC), the posterior cingulate, the retrosplenial, and lateral posterior parietal cortex (PPC) (Buckner et al., 2005). These abnormalities are accompanied by an initial disruption of medial frontoparietal functional connectivity, as evidenced by alterations of the so-called default mode network (DMN), for which the PC is a crucial node (Buckner et al., 2008; Raichle et al., 2001). The disconnection of the PC precedes (and potentially contributes to) regional brain atrophy, which becomes prominent at later disease stages (Gili et al., 2011). Indeed, AD patients” frequently exhibit reduced PC cortical thickness, “abnormal activity during memory task performance, and decreased functional connectivity (Chen et al., 2017). This is significant as PC activity is essential for episodic memory retrieval (Lundstrom et al., 2005; Wagner et al., 2005). Consequently, the PC is a vulnerable region for the transitional stage towards dementia and may represent an ideal target for tailored interventions aimed at mitigating AD-related memory decline” (Koch et al., 2018).

# 6. Study: Mapping the neurophysiological Precuneus connectivity in Alzheimer's Disease patients from group to individual level: a TMS, EEG, and MRI integrated approach

## 6.1 Abstract

Alzheimer's Disease is a well-known neurodegenerative pathology. However, the urgency to advance our understanding of the underlying neurophysiology is still high. The patients present shared symptoms and characteristic lines to the pathology. Even though the variability among them is enormous. AD is a neurological condition that gets more severe over time but not in an established progression. In some cases, it can speed up the progression of the neurodegeneration. So, the principal aim of recent research concerns recognizing the early stages of the pathology as soon as possible and characterizing the patient's condition at the individual level to optimize the treatment to slow down the degeneration's progress. This study explored the structural and functional connectivity and their correlation of the precuneus region in AD patients with an integrative approach with the aim to characterize at individual level the neurophysiology of the pathology. The connectivity information was collected using functional and structural magnetic resonance imaging, diffusion tensor imaging, concurrent transcranial magnetic stimulation, and electroencephalography. To characterize functional connectivity, we have recorded TMS-EEG from a nine-point grid reconstructed over the Precuneus region to map the activation more accurately. The signal propagation recorded from all these points has been compared at the group level with a set of comparisons with both functional and structural connectivity measures. Our results suggest various roles played by the different points composing the grid in modifying connectivity in the resting state AD scenario. Moreover, the individual inspection of the source activation within the nine-point Precuneus grid lets us depict a carefully individualized profile of activation and connectivity. The findings from our study indicate that the proposed integrated approach enabled us to identify a connection between the functional and structural connectivity within the Default Mode Network. Thus, a relationship between the cortical brain regions that are functionally linked and the structural path that connects them is proved. Moreover, these results are pioneering evidence in moving from group to individual brain connectivity characterization.

## 6.2 Introduction

Alzheimer's disease (AD) is recognized as the leading cause of dementia globally (Mayeux & Stern, 2012). Despite various proposed pathophysiological models, the exact etiology of AD remains elusive, and brain-related dysfunctions are not yet fully comprehended. Examining brain connectivity in AD patients has emerged as one of the most promising approaches to exploring the disease's neurophysiological and cognitive impairments. Recent studies have suggested that synaptic function loss might be an early occurrence preceding neuronal degeneration. This synaptic mechanism impairment "could play a crucial role in the onset of cognitive dysfunction in" AD by disrupting large-scale connectivity (Casula et al., 2022; Koch et al., 2018, 2022). Cognitive damage becomes apparent only after a significant synaptic loss has occurred in susceptible brain regions (Reddy et al., 2010). AD results in connectivity dysfunction, potentially affecting specific resting-state brain networks (RSNs). Metabolic "18F-fluorodeoxyglucose positron emission tomography (FDG-PET) and functional Magnetic Resonance Imaging (fMRI)" data have revealed a notable dysfunction of the Default Mode Network (DMN) (Buckner et al., 2008; Dennis & Thompson, 2014; Raichle et al., 2001; Wu et al., 2011). Core AD symptoms, such as memory deficits, have been attributed to this DMN brain connectivity disruption (Koch et al., 2018; Mevel et al., 2011; Morris, 1996; Veldsman et al., 2017). In particular, the Precuneus (PC) is leading in DMN (M E Raichle et al., 2001; Marcus E Raichle et al., 2015), and its alteration is crucial in AD (Maiella et al., 2024). To date, "it has not been possible to directly quantify the relationship between synaptic functioning (or dysfunction)" within specific brain networks like the DMN in vivo in AD patients (Koch, 2020). Various techniques, including FDG-PET (Ding et al., 2019), fMRI (Sperling, 2011), and electroencephalography (EEG) (Horvath et al., 2018), have been employed to investigate the connection between "synaptic dysfunction and network connectivity in AD" patients. However, these methods "provide only an indirect assessment of network dysfunction, limited by their low temporal resolution" (Koch, 2020). Most evidence "regarding brain connectivity has been obtained from stand-alone neuroimaging methods" (Esposito et al., 2020; see Chapter 3). We propose to overcome the limits of using a stand-alone approach with an integrative approach (see Chapter 3). The integrative approach is "composed of structural and functional magnetic resonance imaging (MRI and fMRI), diffusion tensor imaging (DTI), and combined transcranial magnetic stimulation and electroencephalography (TMS-EEG)" (Esposito et al., 2020). Methodological integration is a promising approach to obtaining connectivity

information with different characteristics, which can be helpful in a comprehensive scenario (see Chapter 3).

This study employed an innovative multimodal technique to investigate neural signal propagation using a nine-point grid over the Precuneus in Alzheimer's disease (AD) patients. We aimed to gain new insights into the disease's pathophysiology and illuminate this critical aspect, moving from group characterization to individual description. We utilized a combination of transcranial magnetic stimulation and electroencephalography (TMS-EEG). This promising method directly examines local and widespread cortical dynamics by recording post-synaptic potentials following TMS-induced depolarization. By delivering a series of TMS pulses to the nine-point precuneus (PC) grid, a central hub of the DMN, we sought to determine how neural signals propagated from the stimulation site throughout the network in each patient. We then incorporated functional and structural MRIs to contextualize these neurophysiological signals within each individual's anatomical and functional network structure.

## 6.3 Materials and Methods

### 6.3.1 Experimental Design and Participants

The experimental protocol for this study was approved by the Santa Lucia Foundation IRCCS (Protocol number: CE/2023_013). It was conducted by the ethical standards of the 2013 Declaration of Helsinki and the International Conference on Harmonization Good Clinical Practice guidelines. As the patients entered the study, they gave their written informed consent. Fifteen patients (ten females, mean age 70.8 ± 8.4; five males, mean age 76 ± 8.5) "with a diagnosis of mild to moderate dementia due to AD were enrolled after assessing their compatibility with MRI and TMS-EEG equipment through a screening questionnaire" (Rossi et al., 2011; Rossini et al., 2015; Sammet, 2016). Patients were recruited internally within the Santa Lucia Foundation IRCCS (Rome, Italy). Their "recruitment was performed according to current diagnostic criteria for prodromal AD" (Dubois et al., 2016) and following the previous procedure of Koch and colleagues in 2018. A specific " refers to the early symptomatic phase of AD, characterized by episodic memory loss in the presence of AD pathology as supported by CSF or imaging biomarker evidence" (Koch et al., 2018). "All AD patients had to be cognitively intact before cognitive impairment" (mean MMSE = 19.4 ± 5.8) (Koch et al., 2018). "The lumbar puncture was performed in all patients to confirm the typical CSF profile of AD pathology, i.e., reduced amyloid β1-42 concentrations and increased levels of total- and phosphorylated-tau. Major systemic and psychiatric disorders, other neurological conditions, and signs of concomitant cerebrovascular disease on MRI scans were carefully investigated and excluded in all patients" (Koch et al., 2018).

The study comprises three sessions in which the MRI acquisition and two TMS-EEG recordings were performed, respectively (Table 1). For the third session, the sample was reduced to ten (six females, mean age 72.4 ± 9.9; four males, mean age 74.5 ± 9) due to subjects dropping off. Structural, functional, and diffusion-weighted imaging were recorded at rest for each subject during the MRI session. The two TMS-EEG sessions consist of two of the same acquisitions performed at a distance of one month. TMS was applied over a 9-point precuneus stimulation grid concurrent with multichannel EEG recording in the TMS-EEG acquisition. Recording coordinates were defined from MRI data and used for neuronavigation during the combined acquisition. Each subject underwent nine blocks within the experimental session. Subjects wore earplugs and were seated in comfortable

armchairs with their eyes open. All the blocks "were instructed to fixate a white fixation cross on a computer screen at a distance of 70 cm" (Esposito et al., 2022).

| **Experimental Design** | | |
|---|---|---|
| 1st Session | 2nd Session | 3rd Session |
| MRI Acquisition | TMS-EEG | TMS-EEG |
| • Structural<br>• Resting fMRI<br>• DWI | • 9 grid points over Precuneus<br>• 64 EEG channels<br>• 60 pulses at adjusted TEP threshold<br>• ISI random 2-4 s | |

Table 1 - The table represents the main characteristics of the experimental design.

6.3.2 MRI

MRI data were acquired on a Siemens PRISMA scanner with a 64-channel head-coil (Siemens, USA) before the neuromodulation protocols. The MRI procedure is the same as described by Mencarelli and colleagues in 2022. "The structural imaging was acquired using high-resolution T1-weighted (T1) anatomical images obtained through a 3D-MPRAGE sequence (TR=2200ms, TE=2.39 ms, TI=800ms, flip angle (FA)=12°, thickness=1mm, imaging matrix= 240 × 256; acquisition duration: 5.38''), whereas the functional MRI images were acquired using standard echo-planar blood oxygenation level-dependent (BOLD) imaging (TR=3200ms, TE=25 ms, flip angle (FA)=90°, thickness=2.5mm, gap=2.5mm, acquisition duration: 6.46''). Subjects were instructed to rest and not to focus their thoughts on any particular topic, not to cross their arms or legs, and to keep their eyes open. An investigator expert in MRI checked both resting-state functional connectivity (rs-FC) maps of the Precuneus and structural MRI data (i.e., T1-weighted images) to identify individual Precuneus hotspots based on ad-hoc criteria. In particular, the stimulation site was defined as the closest to the local maxima of the rs-FC cluster, being on the top of a cortical gyrus and representing the shortest perpendicular path connecting the stimulating TMS coil on the scalp and the cortex. Based on best judgment, the resulting set of coordinates was picked as the individual stimulation site. The individual set of coordinates was then transformed using a non-linear transformation to reconstruct the target in the individual brain

spaces. Lastly, the individualized target was marked in the subject's anatomical MRI and loaded into our neuronavigation system." (Mencarelli et al., 2022).

### 6.3.3 EEG

The EEG was acquired using a TMS-compatible EEG equipment (Bittium Neurone system from Bittium Corporation, Finland), with a continuous recording from 60 scalp electrodes (Fp1, Fp2, F3, F4, C3, C4, P3, P4, O1, O2, F7, F8, T7, T8, P7, P8, Fz, Cz, Pz, FC1, FC2, CP1, CP2, FC5, FC6, CP5, CP6, AFz, FCz, F1, F2, C1, C2, P1, P2, AF3, AF4, FC3, FC4, CP3, CP4, PO3, PO4, F5, F6, C5, C6, P5, P6, AF7, AF8, FT7, FT8, TP7, TP8, PO7, PO8, CPz, POz, Oz) positioned according to the 10/20 International System. The ground electrode was placed at AFz. The online reference was placed on the tip of the nose. Horizontal and vertical eye movements were detected by recording the electrooculogram (EOG). All the electrodes were TMS-compatible Ag/AgCl-coated electrodes mounted on an elastic cap (BrainCap TMS, Brain Products GmbH, Germany). This sensor is built to avoid overheating the electrodes near the stimulating coil. The EEG and EOG signals were band-pass filtered at 0.1-1000 Hz and digitalized at a sampling rate of 5 kHz. The impedance was kept below 5 kΩ for all skin/electrode interfaces.

### 6.3.4 TMS

Single-pulse TMS was carried out using a Magstim Rapid2 magnetic biphasic stimulator connected with a figure-of-eight coil with a 70-mm diameter (Magstim Company, Whitland, UK). Each TMS-EEG session consisted of 60 single pulses applied at a random inter-stimulus interval (ISI) of 2–4sec. TMS was applied over nine different points, which comprised a grid of equidistant 1.5cm over the Precuneus region. The grid (Figure 9) is calculated on each patient's scalp. The starting point coordinates (labeled A) come from the Precuneus hotspots from the MRI analysis. A grid is calculated on the scalp, positioning the other eight vertices at a distance of 1.5 cm from each other, forming a square over the Precuneus area. All the vertices are labeled with letters from B to I from the left top corner to the right bottom corner. All the point coordinates are used for the concurrent TMS-EEG neuronavigation.

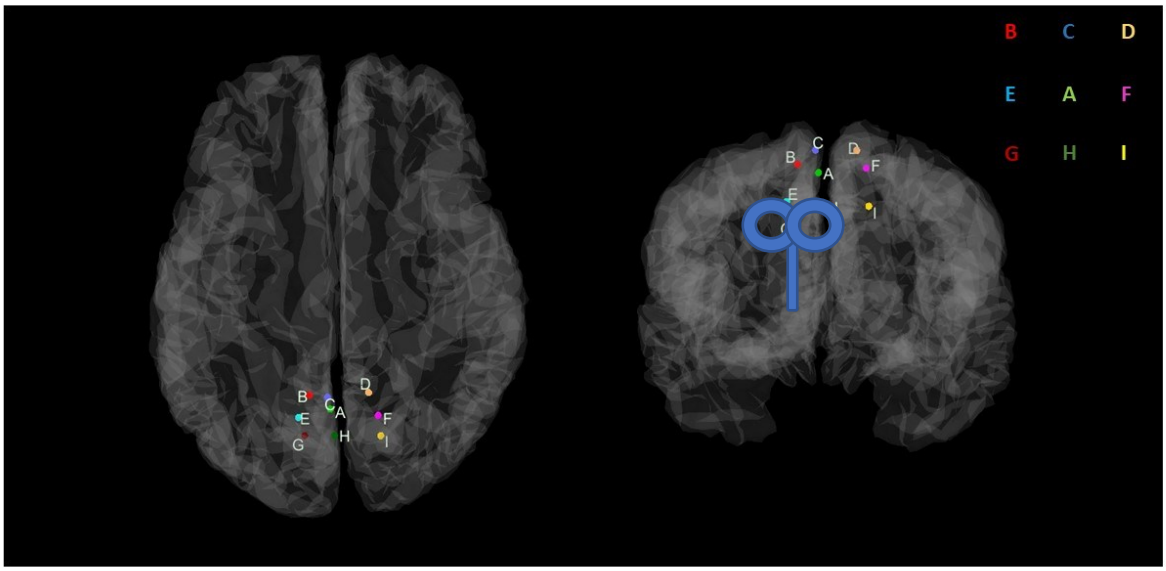


Figure 9 – Representation of the 9-point grid over the Precuneus region.

The coil position and orientations (Figure 9) were continuously monitored using the SofTaxic Neuronavigation System (E.M.S. srl Company, Bologna, Italy) to ensure high reproducibility across neurophysiological assessments. The order of stimulation of either point was counterbalanced with a permutation. The intensity of stimulation of single-pulse TMS was set through the online inspection of the TEPs amplitude (see review Pavon et al., 2023). Before recording each point of the grid, we visually monitored the amplitude of the components in the first 50 ms after the TMS pulse on an average of 20 trials. To maintain a peak-to-peak amplitude of 6-8 μV. The mean intensity TMS value was 72.9 ± 9.4 for the first TMS-EEG session and 71.1 ± 10.4 for the second TMS-EEG session.

## 6.4 Data Pre-processing

### 6.4.1 Structural and Functional MRI

SPM12 (Statistical Parametric Mapping), CONN, and MATLAB 2018a (MathWorks, MA, USA) software were used to pre-process datasets. The following preprocessing (Mencarelli et al., 2024) steps were "applied to the BOLD images: discarding of the first three volumes to allow for steady-state magnetization and stabilization of participant status; slice timing; realigning to correct for head motion; co-registration to structural images; segmentation; nonlinear normalization to the Montreal Neurological Institute (MNI) template brain; voxel resampling to an isotropic 3 × 3 × 3 mm voxel size; smoothing with an isotropic Gaussian kernel (full-width at half maximum, 8 mm). Structural images were co-registered and segmented to the mean volume of functional images". To minimize the impact of the MRI scanner's increasing temperature, linear trends were eliminated. Additionally, all functional volumes underwent bandpass filtering at $0.01\ \text{Hz} < f < 0.08\ \text{Hz}$ to mitigate low-frequency fluctuations. Finally, we "regress out potential confounding signals, like physiological high-frequency respiratory and cardiac noise, from grey matter voxels' BOLD time course using the Compcorr algorithm (Whitfield-Gabrieli & Nieto-Castanon, 2012) to reduce artificial negative correlation and provide adequate filtering of the data".

### 6.4.2 Selection of the first point of the Precunes-grid

Functional connectivity maps were created using a seed-based approach to identify the optimal precuneus stimulation site. The DMN regions were derived from the Harvard-Oxford atlas available in the Conn Functional Connectivity Toolbox, and the precuneus was defined as the seed region (Whitfield-Gabrieli & Nieto-Castanon, 2012). Seed-to-voxel correlation maps were computed for each participant by correlating the average BOLD signal of the precuneus seed with every voxel within the DMN subregions, resulting in rs-functional connectivity (rs-FC) maps of precuneus-DMN connectivity strengths. Local maxima were then identified as the precuneus locations showing peak correlation values within the DMN rs-FC map. "The optimal stimulation location was chosen by an MRI expert based on several criteria: (1) it needed to be the closest to the local maxima of the precuneus, (2) being located on top of a cortical gyrus, and (3) having the shortest perpendicular path from the scalp to the cortex" (Momi et al., 2020). This approach ensured that the chosen site represented the most robust functional connectivity within the DMN while also being

accessible for TMS. The final coordinates were then transformed to reconstruct the stimulation point within the subject-specific brain space. This was done utilizing a non-linear transformation of the precuneus MNI coordinates (x, y, z: 0, -62, 64) through a custom script using the FMRIB Software Library (FSL).

### 6.4.3 Diffusion and Tractography

A multishell diffusion scheme was applied, and the b-values were 300,1000, and 2500 s/mm². The number of diffusion sampling directions was 8, 32, and 71, respectively. The in-plane resolution was 1.793 mm. The slice thickness was 1.80 mm. 11 PA encoding and 1 AP encoding b0 images were used to estimate susceptibility using FSL top-up. FSL's top-up was used to correct susceptibility distortion using DWI acquired from one phase encoding direction. Restricted diffusion imaging (Yeh et al., MRM, 77:603–612 (2017)) was employed to measure the restricted diffusion. The reconstruction of diffusion data utilized generalized q-sampling imaging (Yeh et al., 2010), applying a diffusion sampling length ratio of 1.25. DWI with a b-value below 1750 s/mm² was used to calculate tensor metrics.

### 6.4.4 Structural and Functional Connectivity Measures

We have extracted an index from tractography to represent the structural connectivity of the Cingulum and the Middle Longitudinal Fasciculus (MdLF). The “index was an extracted tensor-derived quantitative measure of microstructural diffusivity for each connection, the Fractional Anisotropy (FA)” (Esposito et al., 2022). Fractional anisotropy (FA) measurements provide numerical indicators of axonal health by assessing water anisotropy along the axon. These values offer a comprehensive measure of diffusion directionality and exhibit high sensitivity to microstructural alterations.
Instead, three regions of interest (ROI) have been selected for the functional resting state activity: the medial prefrontal cortex (MPFC), the left and right temporal pole, and the hippocampus.

### 6.4.5 TMS-EEG

TMS-EEG data were preprocessed offline using TESA (Rogash et al., 2017) using a custom script in a MATLAB environment (MathWorks Inc., Natick, MA, 2021b). Data were segmented into epochs starting 1.5 s before the TMS pulse and ending 1.5 s after the pulse. A cubic interpolation was applied from 1 ms before to 10 ms after the TMS pulse to remove TMS-induced artifacts. Afterward, a FastICA decomposition was performed to remove the residual of the TMS-pulse muscular artifact. Next, the signal was downsampled from 5000 Hz to 1000 Hz. Afterward, a high-pass filter at 1 Hz was applied to the continuous data. Subsequently, the low-pass filter at 80 Hz and a notch filter at 50 Hz were applied to the data. Afterward, all the epochs were visually inspected, and the noisy EEG epochs were rejected. Then, physiological and TMS-related artefactual components were detected using FastICA and removed based on their scalp distribution, frequency, timing, and amplitude. So, the segmented signal was re-referenced to averaged, and residual artifacts were removed with a second rejection. Then, the signal was imported into Fieldtrip (Oostenveld et al., 2011) and segmented, starting 100 ms before the TMS pulse and ending 400 ms after it. A baseline correction was applied before 100 ms to -1 ms. Pre-processed EEG data were imported in Brainstorm (Tadel et al., 2011) (V. 05-Nov-2024), software running in a MATLAB environment (MathWorks Inc., Natick, MA, Version R2021B) to perform source analysis to reconstruct the topographical origins of the TMS-EEG signals (Figure 10).

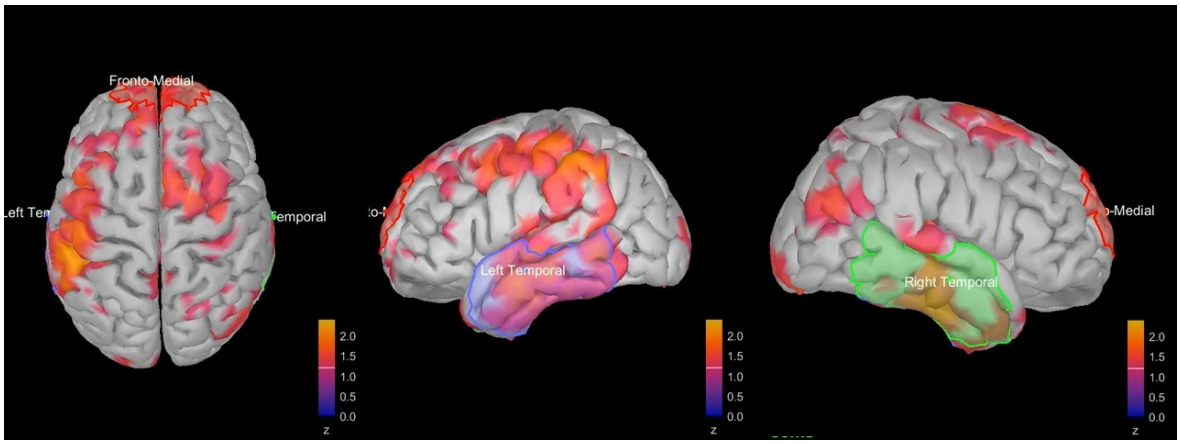


Figure 10 - Selection of the three scouts (Fronto medial, Left, and Right Temporal lobes) from which we have extrapolated the source propagation.

## 6.5 Statistical Analysis

The statistical analysis was performed with FieldTrip (Oostenveld et al., 2011), a MATLAB toolbox, through a custom pipeline. Non-parametric, cluster-based permutation statistics were conducted to correct for multiple comparisons. For the statistical testing, the ft_timelockstatistics and ft_sourcestatistics function was employed. Moreover, the general linear model and correlations were run with Jamovi software (version 2.3.28) (https://www.jamovi.org).

Firstly, it was assessed if the two TMS-EEG sessions differed in the sensor space and the source space. The comparison involved all the electrodes for each stimulation condition for the time window of interest from 11 to 100 ms after the TMS pulse for the time domain and from 0 to 250 ms for the source domain, respectively. The definition of the time window is based on evidence that defines this interval as crucial for the signal spreading into the homologous regions in the opposite hemisphere (Chung et al., 2015; Ilmoniemi et al., 1997; Parks et al., 2012) and to avoid artifacts, i.e., the auditory evoked potentials at 100 ms (Conde et al., 2019; Nikouline et al., 1999; Ter Braack et al., 2015). Initial one-sample t-tests were conducted to identify significant time points and electrodes. Clusters were formed by grouping adjacent significant samples with t-values exceeding a threshold corresponding to an uncorrected p-value of .05. This process was carried out separately for positive and negative t-values in a two-tailed test. To be included in a cluster, a significant sample required at least one neighboring significant sample in both time and space (electrodes). Each electrode's spatial neighborhood encompassed all electrodes within approximately 5 cm, resulting in an average of 6.3 neighbors (minimum 3, maximum 8) and a median of 7 neighbors per electrode. Cluster statistics were generated by summing the t-values within each cluster. This procedure was repeated 2500 times to calculate the Monte Carlo estimate of significance probabilities through permutations.

Subsequently, a group-level analysis of signal propagation differences was performed on the nine-point grid at baseline. A linear mixed model was employed, with source activation as the dependent variable, stimulation grid points, scout areas, their interaction as fixed effects, and subjects as a random effect. Post hoc comparisons were conducted to investigate differences among all grid points.

Then, to characterize a subject-level distribution of activity propagation among the nine-point grid, the z-scored values of the heatmap activation of the source activation have been plotted. The same has been done for the amplitude of the early three peaks (P30, N45, P65; see Casula et al., 2022) of the TEPs recorded from the Pz electrode. Further correlation

analysis (Pearson's coefficient) has been done to explore relations between cortical reactivity and signal propagation.

Lastly, the correlation (Pearson's coefficient) between the nine-point grid signal propagation, the functional MRI activity, and the FA values of the Cingulum and the MdLF was assessed.

## 6.6 Results

### 6.6.1 TMS-EEG recording comparison

#### 6.6.1.1 Sensor space

A statistical comparison performed on all electrodes in the time window from 11 to 100 ms after the TMS pulse did not reveal any differences between the two TMS-EEG sessions (all ps > 0.05, Figure 11 and Figure 12).

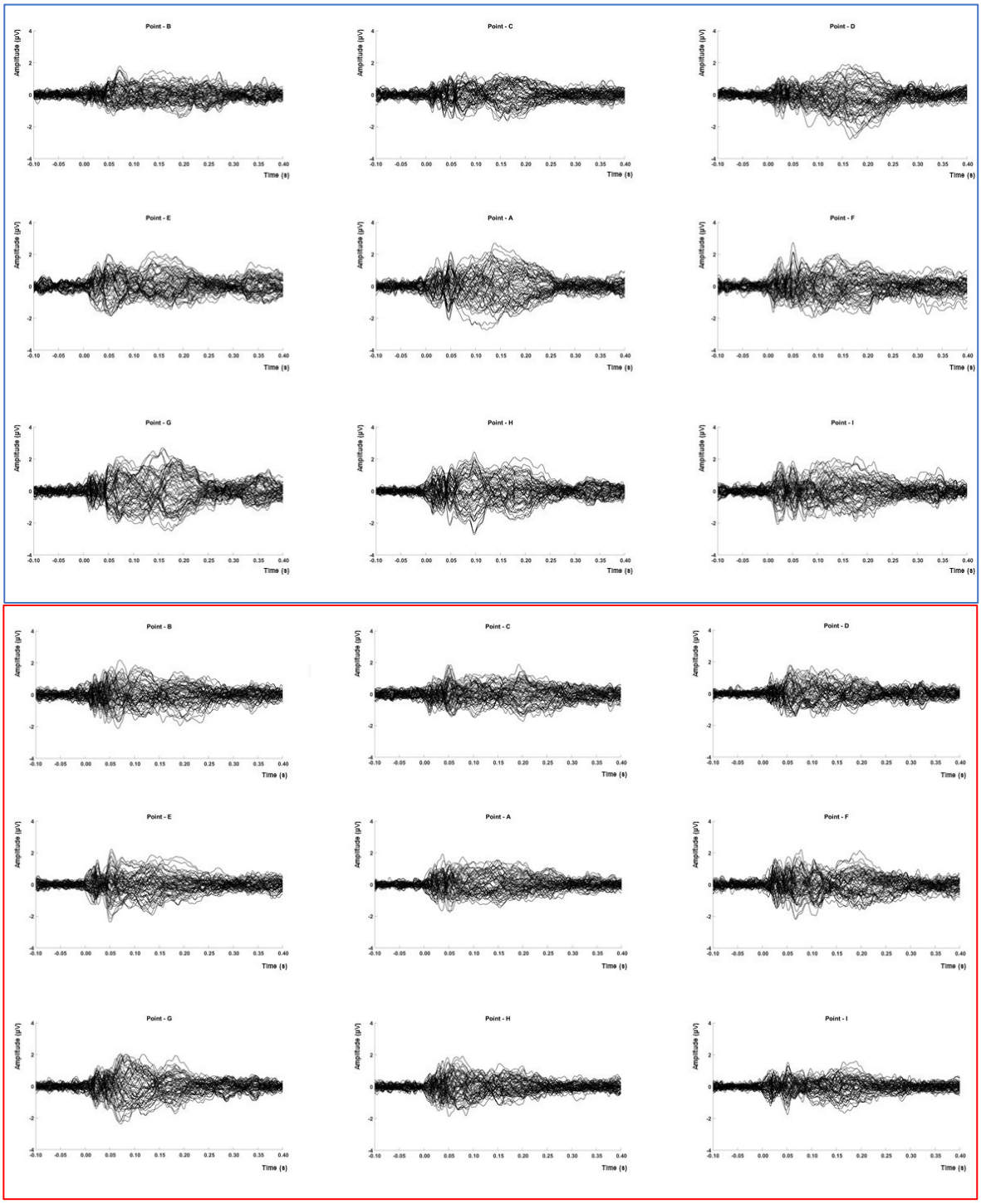


Figure 11 - Butterfly plot of all channels for each point of the nine-point grid is plotted. Blue= first TMS-EEG session, Red= second TMS-EEG session

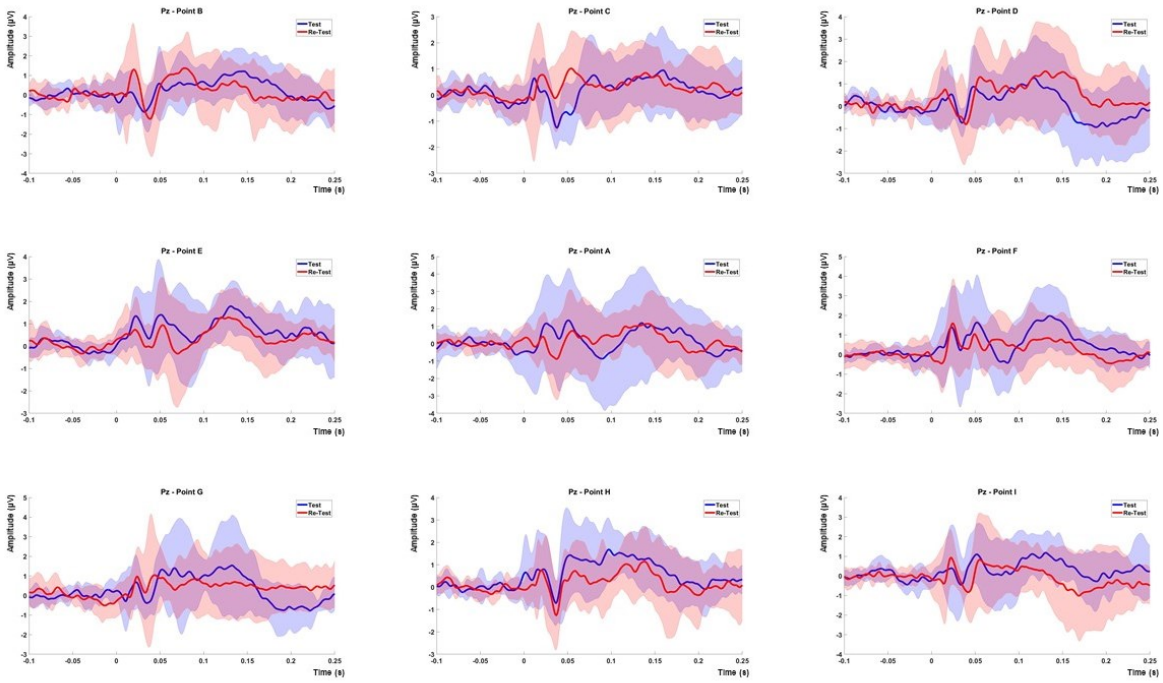


Figure 12 - The Pz electrodes for each stimulation condition are plotted. No significant results emerged. Blue = first TMS-EEG session. Red = second TMS-EEG session.

6.6.1.2 Source space

A statistical comparison performed on all electrodes in the time window from 0 to 250 ms after the TMS pulse did not reveal any differences between the two TMS-EEG sessions (all ps > 0.05, Figure 13).

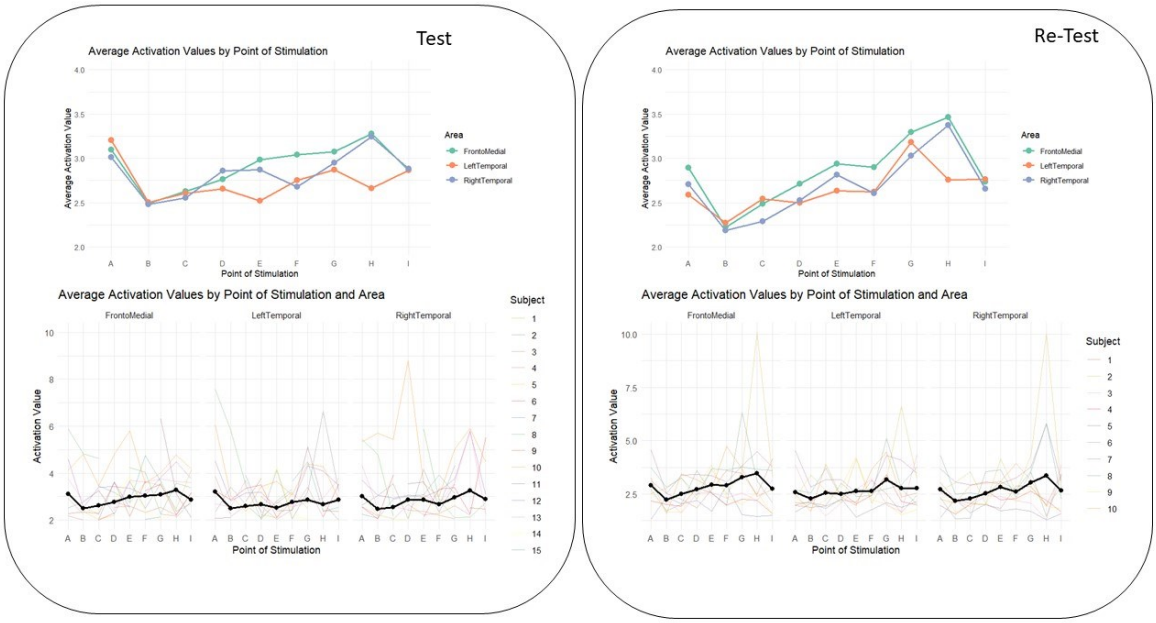


Figure 13 - The source activation for each point of the grid is plotted and averaged for each extrapolated source scout (upper section) and each patient activity (lower section). No significant results emerged.

6.6.2 Nine-point grid signal propagation difference

The linear model assessed source activation as the dependent variable, with the ROIs (mPFC, left-TL, right-TL) and stimulation points as fixed effects. Significant effects and tendencies were observed for some stimulation points compared to reference Point A (see Table 2).

| Effect | *t* | *p* |
|---|---|---|
| B-A | -2.9 | 0.004 |
| C-A | -2.4 | 0.017 |
| D-A | -1.6 | 0.103 |
| E-A | -1.5 | 0.139 |
| F-A | -1.3 | 0.184 |
| G-A | -0.7 | 0.505 |
| H-A | -0.2 | 0.831 |
| I-A | -1.1 | 0.267 |

Table 2 - P-values of the GLM

Moving from the top to the bottom of the nine-point grid reduces the difference in source activation respect to point A (see Figure 14).

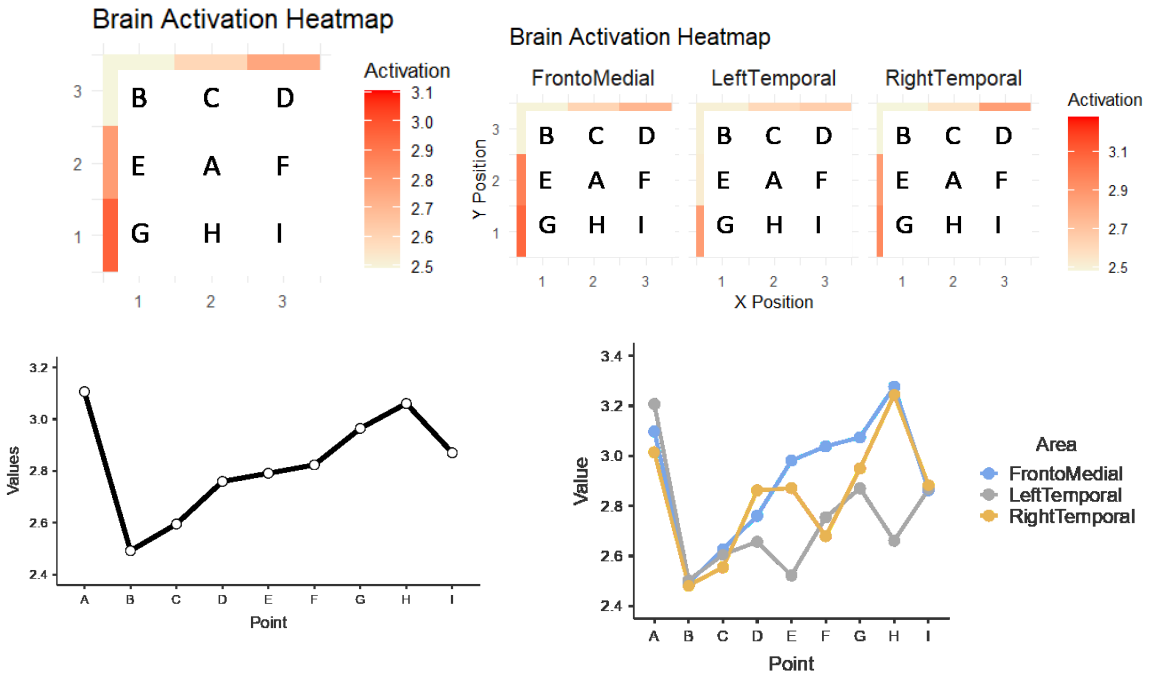


Figure 14 - the upper row, the heatmap of the source activation among the nine-point grid is plotted. The linear graph of the activity distribution is shown in the lower row. On the left, the average of the source activation is plotted; on the right, the activation of each source ROI is plotted.

Post hoc t-tests have evaluated the differences among all the point combinations. The correlations have not been corrected (see Table 3).

Post Hoc Comparisons - Point

| Comparison | | | | | | | |
|---|---|---|---|---|---|---|---|
| Point | | Point | Difference | SE | t | df | p |
| A | - | B | 0.6142 | 0.212 | 2.895 | 364 | 0.004 |
| A | - | C | 0.5110 | 0.212 | 2.408 | 364 | 0.017 |
| A | - | D | 0.3465 | 0.212 | 1.633 | 364 | 0.103 |
| A | - | E | 0.3148 | 0.212 | 1.484 | 364 | 0.139 |
| A | - | F | 0.2826 | 0.212 | 1.332 | 364 | 0.184 |
| A | - | G | 0.1416 | 0.212 | 0.667 | 364 | 0.505 |
| A | - | H | 0.0454 | 0.212 | 0.214 | 364 | 0.831 |
| A | - | I | 0.2357 | 0.212 | 1.111 | 364 | 0.267 |
| B | - | C | -0.1032 | 0.212 | -0.486 | 364 | 0.627 |
| B | - | D | -0.2677 | 0.212 | -1.262 | 364 | 0.208 |
| B | - | E | -0.2994 | 0.212 | -1.411 | 364 | 0.159 |
| B | - | F | -0.3316 | 0.212 | -1.563 | 364 | 0.119 |
| B | - | G | -0.4726 | 0.212 | -2.228 | 364 | 0.027 |
| B | - | H | -0.5688 | 0.212 | -2.681 | 364 | 0.008 |
| B | - | I | -0.3785 | 0.212 | -1.784 | 364 | 0.075 |
| C | - | D | -0.1646 | 0.212 | -0.776 | 364 | 0.439 |
| C | - | E | -0.1962 | 0.212 | -0.925 | 364 | 0.356 |
| C | - | F | -0.2284 | 0.212 | -1.077 | 364 | 0.282 |
| C | - | G | -0.3694 | 0.212 | -1.741 | 364 | 0.082 |
| C | - | H | -0.4656 | 0.212 | -2.194 | 364 | 0.029 |
| C | - | I | -0.2753 | 0.212 | -1.297 | 364 | 0.195 |
| D | - | E | -0.0316 | 0.212 | -0.149 | 364 | 0.882 |
| D | - | F | -0.0639 | 0.212 | -0.301 | 364 | 0.763 |
| D | - | G | -0.2049 | 0.212 | -0.966 | 364 | 0.335 |
| D | - | H | -0.3010 | 0.212 | -1.419 | 364 | 0.157 |
| D | - | I | -0.1107 | 0.212 | -0.522 | 364 | 0.602 |
| E | - | F | -0.0323 | 0.212 | -0.152 | 364 | 0.879 |
| E | - | G | -0.1733 | 0.212 | -0.817 | 364 | 0.415 |
| E | - | H | -0.2694 | 0.212 | -1.270 | 364 | 0.205 |
| E | - | I | -0.0791 | 0.212 | -0.373 | 364 | 0.709 |
| F | - | G | -0.1410 | 0.212 | -0.664 | 364 | 0.507 |
| F | - | H | -0.2371 | 0.212 | -1.118 | 364 | 0.264 |
| F | - | I | -0.0468 | 0.212 | -0.221 | 364 | 0.825 |
| G | - | H | -0.0961 | 0.212 | -0.453 | 364 | 0.651 |
| G | - | I | 0.0941 | 0.212 | 0.444 | 364 | 0.658 |

Post Hoc Comparisons - Point

| Comparison | | | | | | | |
|---|---|---|---|---|---|---|---|
| **Point** | | **Point** | **Difference** | **SE** | **t** | **df** | **p** |
| H | - | I | 0.1903 | 0.212 | 0.897 | 364 | 0.370 |

Table 3 – Comparisons report among all the nine points grid.

The significant comparisons are between points A-B (p = 0.004), A-C (p = 0.017), B-G (p = 0.027), B-H (p = 0.008), C-H (p = 0.029), and finally there is a tendency between B-I (p = 0.075). This comparison confirms that the points present an increasing activation moving from the top of the grid to the bottom. The points in the upper row (B and C) differ from the point extrapolated from the MRI analysis (A) and the other posterior points (G, H, I), which do not differ from each other and other points.

### 6.6.3 Subject-level characterization of source propagation

For each patient tested at baseline (Test session, N=15), we have targeted the point of maximum source activation value through the heatmap inspection (Figure 15). We also have plotted the amplitude distribution of the first components in the sensor domain (P30, N45, and P65). The previous analysis had described a group trend among the nine-point grid. However, we have been interested in exploring each patient activity distribution for a subject-level characterization of the point with the maximum source propagation among the grid (see below). The circle highlights the point with the maximum value.

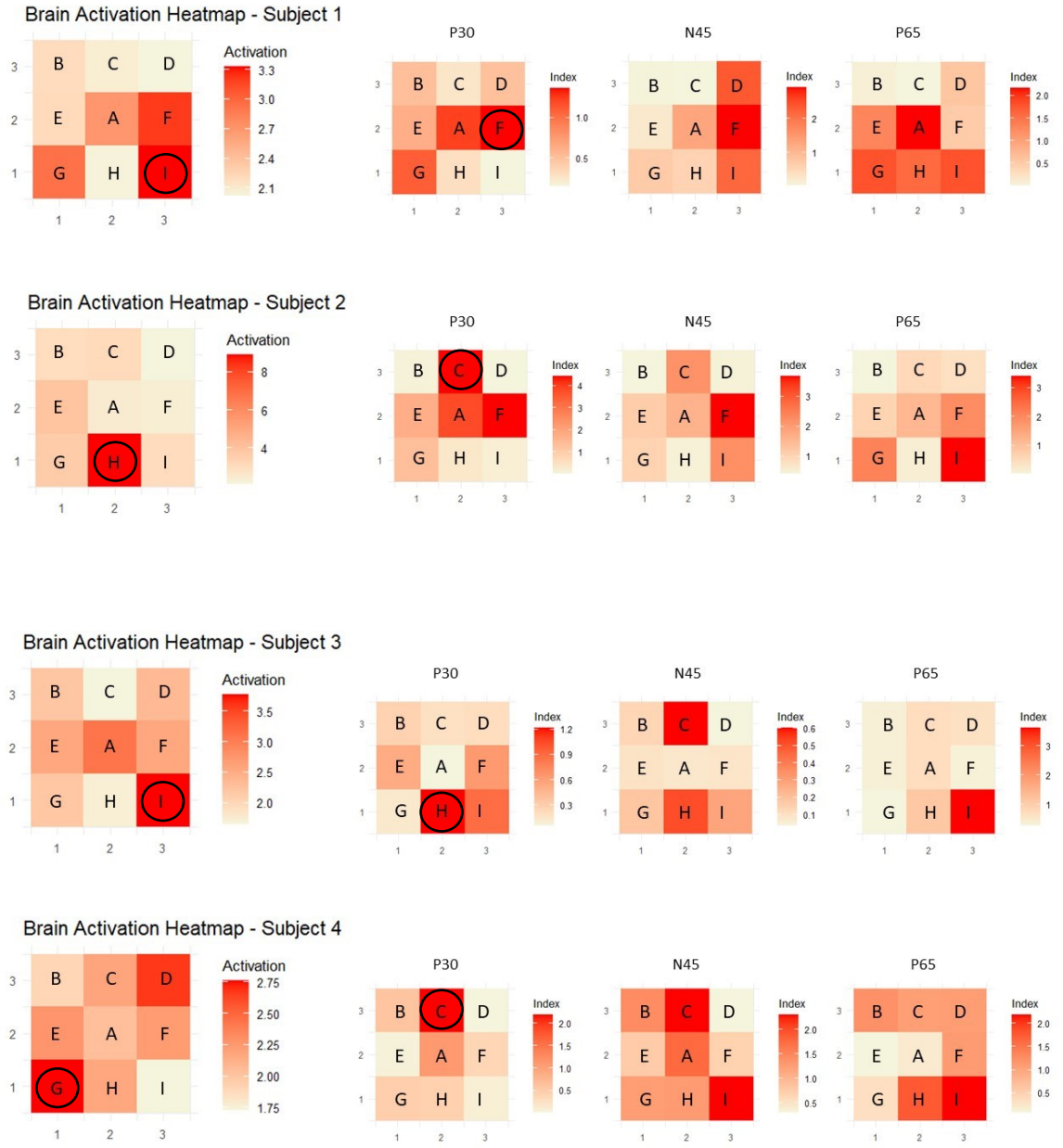

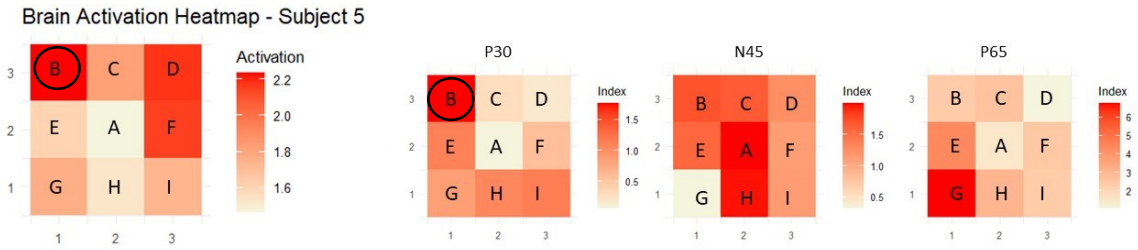
Brain Activation Heatmap - Subject 5
Activation
P30
N45
P65
Index


Brain Activation Heatmap - Subject 6
Activation
P30
N45
P65
Index

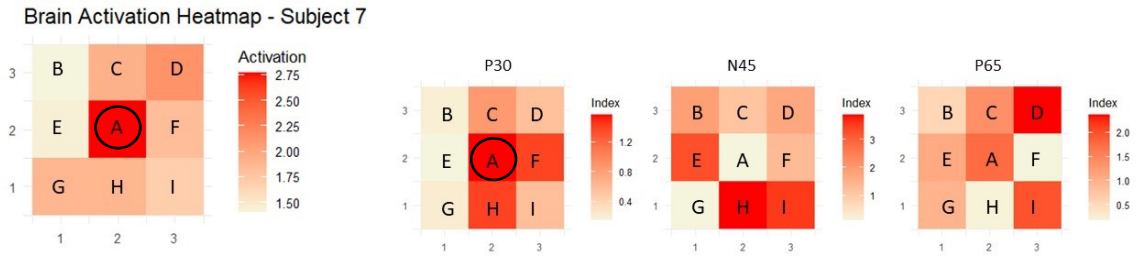
Brain Activation Heatmap - Subject 7
Activation
P30
N45
P65
Index

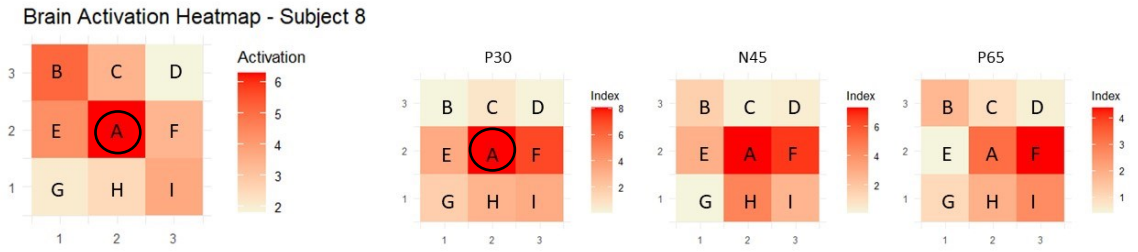
Brain Activation Heatmap - Subject 8
Activation
P30
N45
P65
Index

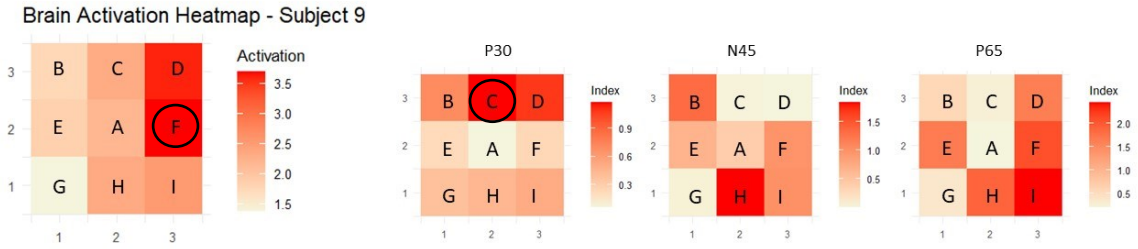
Brain Activation Heatmap - Subject 9
Activation
P30
N45
P65
Index

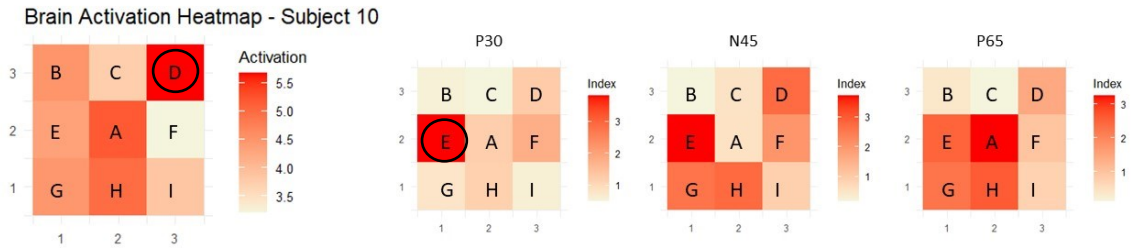
Brain Activation Heatmap - Subject 10
Activation
P30
N45
P65
Index

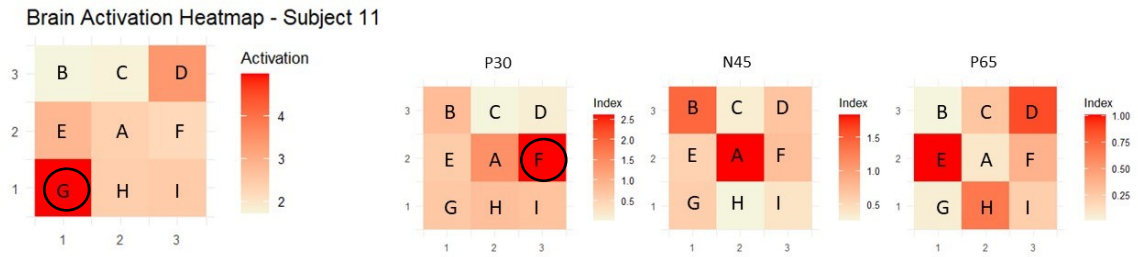
Brain Activation Heatmap - Subject 11
Activation
P30
N45
P65
Index

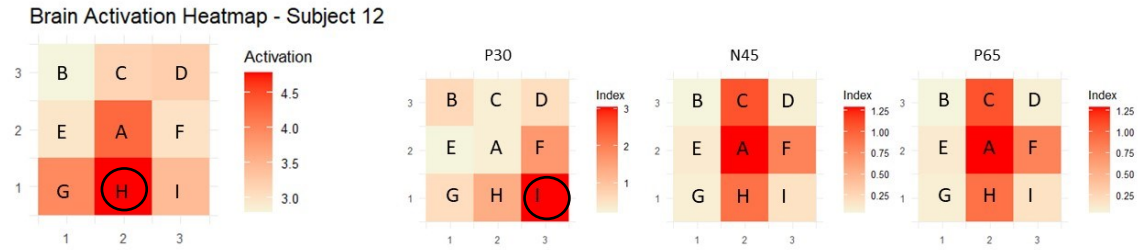
Brain Activation Heatmap - Subject 12
Activation
P30
N45
P65
Index

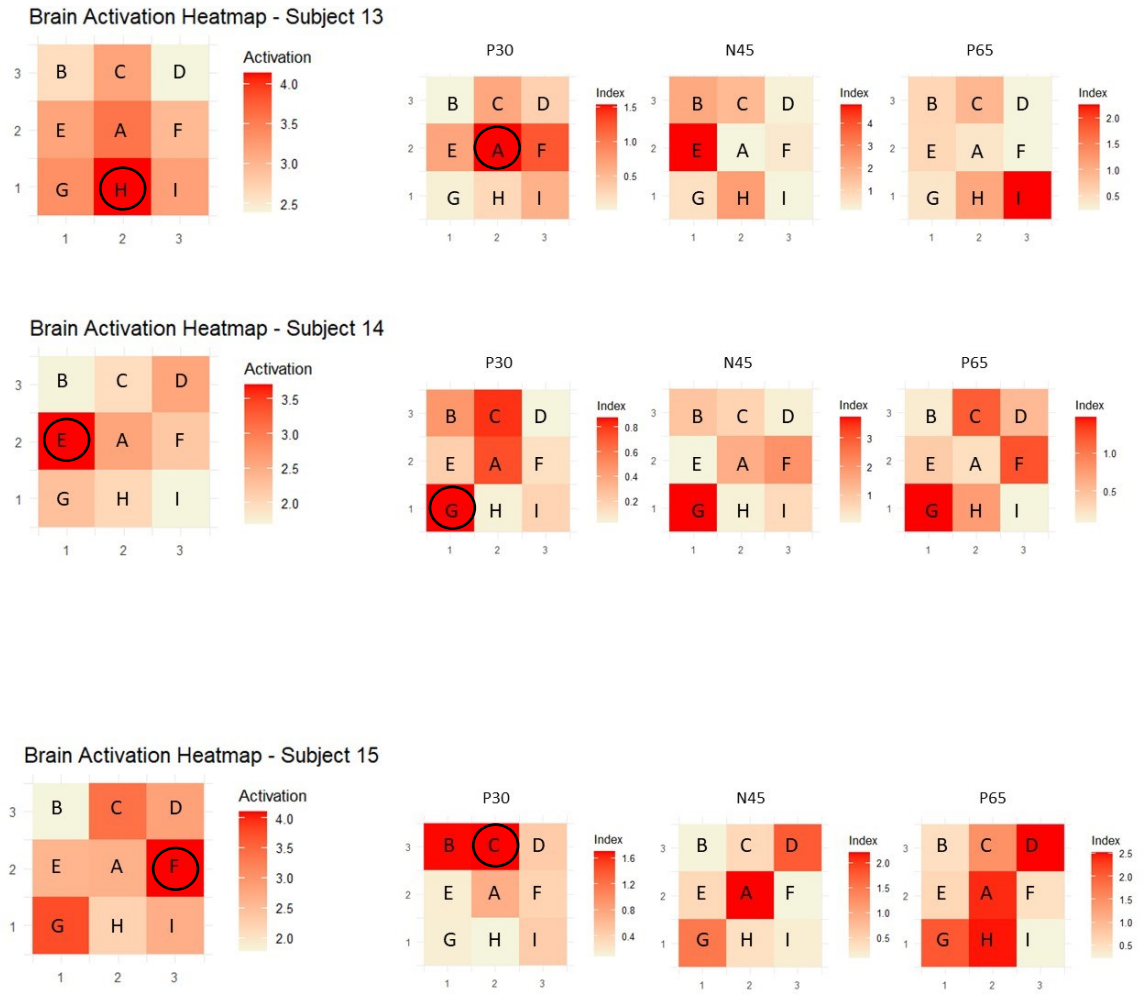


Figure 15 - The source propagation heatmap among each patient's nine-point grid is reported on the left. On the right, three heatmaps describe each TEP component's amplitude distribution among the precuneus grid (P30, N45, P65). The circle highlights the point with the maximum value.

6.6.4 TEPs and Source Correlations

Pearson's correlations revealed significant values for points A, D, E, and I of the nine-point grid. A correlation has been made between the TEP peak amplitude and the source activation. The significant correlations are listed below:

- Point A:

| | **Source Avg** | **Frontal** | **Left Temporal** | **Right Temporal** |
|---|---|---|---|---|
| **P30** | r: 0.629<br>p: 0.012 | r: 0.614<br>p: 0.015 | r: 0.616<br>p: 0.015 | r: 0.564<br>p: 0.028 |
| **N45** | | r: 0.545<br>p: 0.036 | r: 0.514<br>p: 0.05 | |
| **P65** | r: 0.693<br>p: 0.004 | r: 0.672<br>p: 0.006 | r: 0.698<br>p: 0.004 | r: 0.596<br>p: 0.019 |

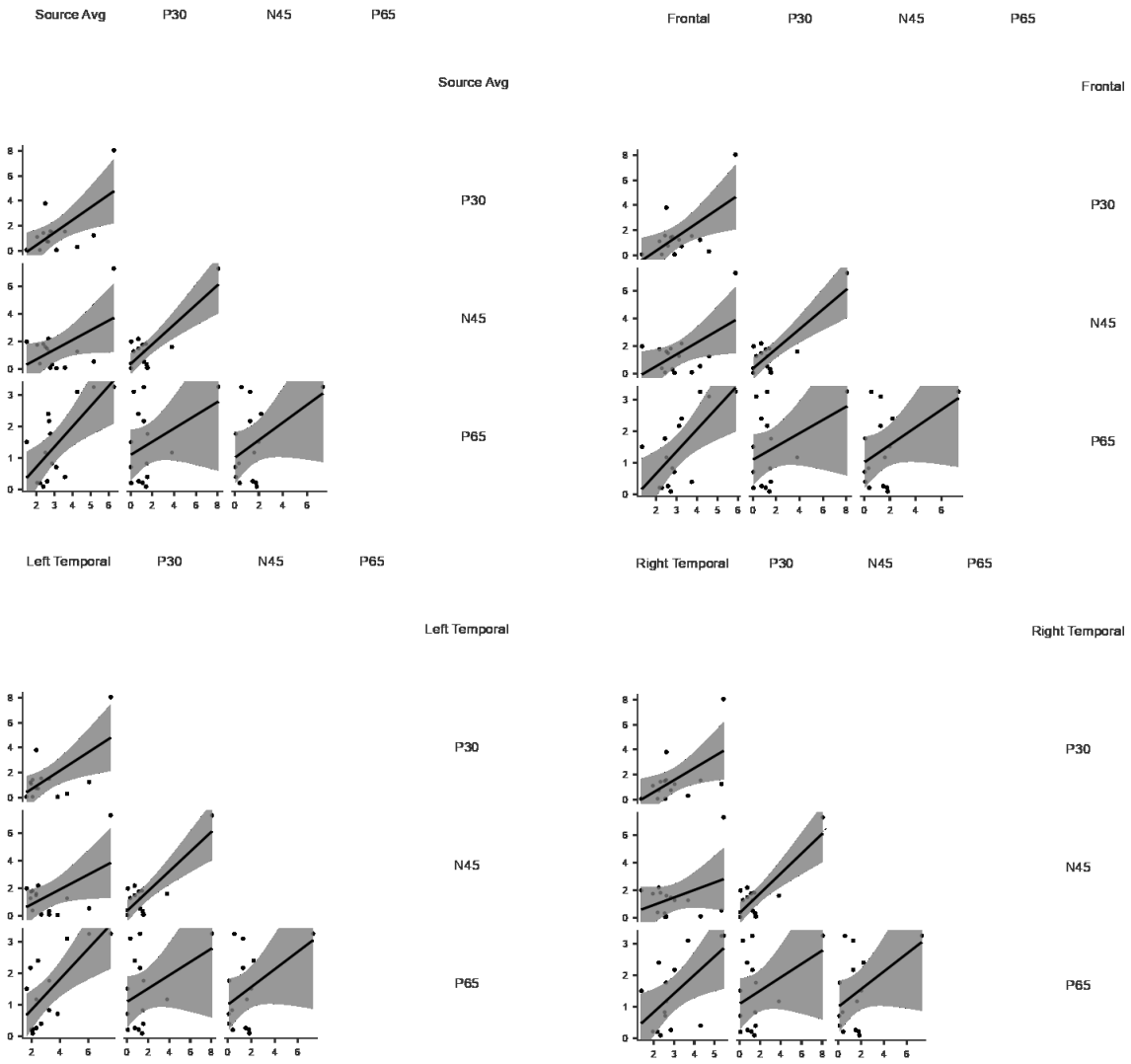

- Point D:

| | Source Avg | Frontal | Left Temporal | Right Temporal |
|---|---|---|---|---|
| **P30** | r: 0.707<br>p: 0.003 | r: 0.569<br>P: 0.027 | r: 0.637<br>p: 0.011 | r: 0.673<br>p: 0.006 |

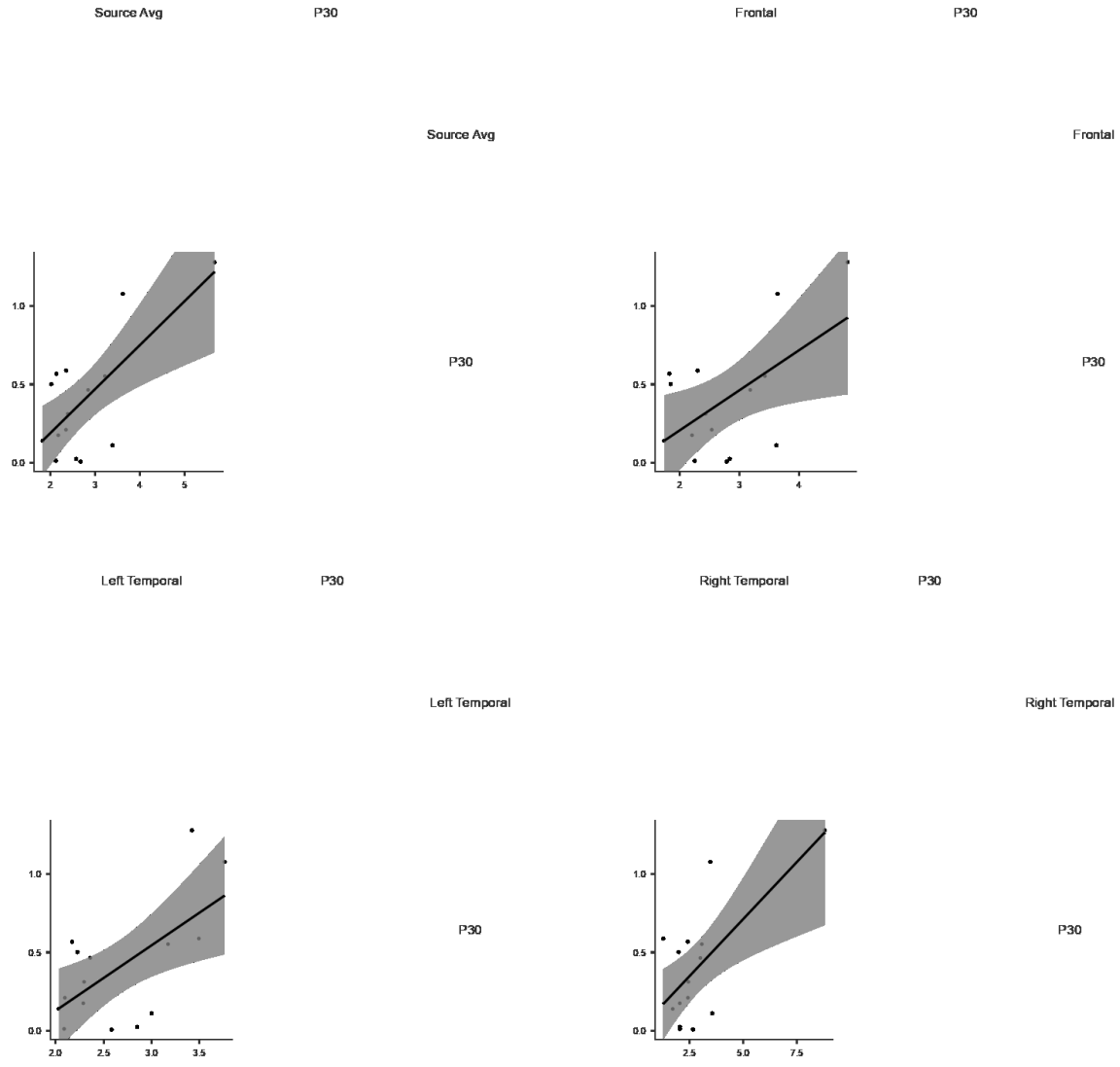

- Point E:

| | Source Avg | Frontal | Left Temporal | Right Temporal |
|---|---|---|---|---|
| **P30** | r: 0.714<br>p: 0.003 | r: 0.742<br>P: 0.002 | | r: 0.677<br>p: 0.006 |

Source Avg P30

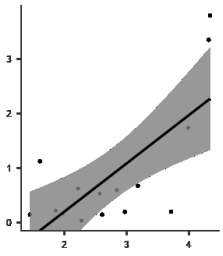


Frontal P30

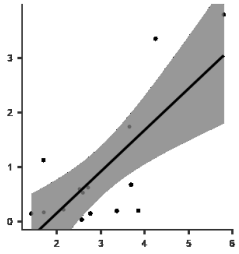


Right Temporal P30

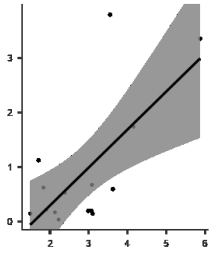

- Point I:

| | Source Avg | Frontal | Left Temporal | Right Temporal |
|---|---|---|---|---|
| **P30** | | | | r: 0.631<br>p: 0.012 |

Right Temporal P30

Right Temporal

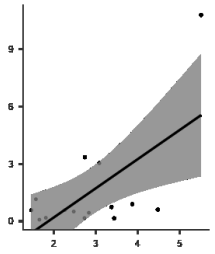


P30

6.6.5 Source Activation and MRI Connectivity Measures correlation

We have selected three points for each patient to explore any relationship between the neurophysiological signal and the MRI data: the points of maximum and minimal activation and point A (the one that emerged from the MRI). We have correlated the source activation with the functional resting state value and FA measures (see above) for those points.

For the correlation with the FA measures, one significant negative correlation (r: -0.717, p: 0.02) has emerged between the frontal source of the point with the maximum activation and the Cingulum's FA (Figure 16 A).

Instead, from the correlation with the functional resting state, one significant positive correlation (r: 0.807, p: 0.005) has emerged between the right temporal source of the point of minimum activation and the hippocampus activity (Figure 16 B).

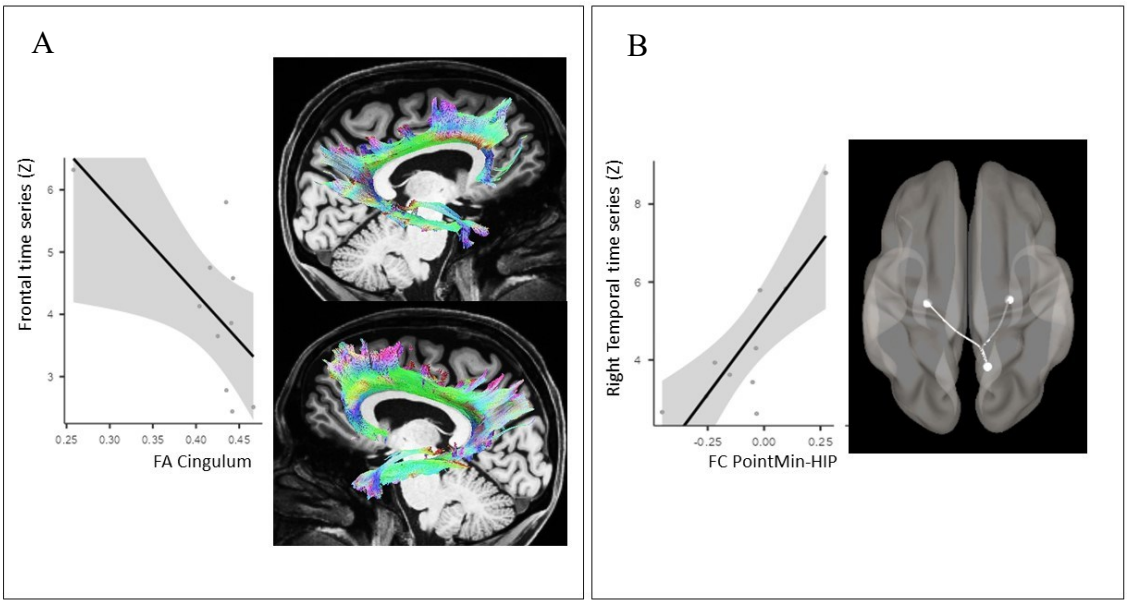


Figure 16 A. The correlation graph is reported on the left, and the reconstructed Cingulum fasciculum is on the right. B. On the left is the reported correlation graph. On the right, the functional activity extrapolated from the MRI.

## 6.7 Further Proposed Investigations

Due to the reported evidence (see above) on the neurophysiological mapping of the Precuneus in AD patients, we will test the behavioral aspect of this functional characterization. As described in the previous paragraphs, memory impairment is the principal prodromal symptom of this neurodegenerative disease. So, guided by the reported results of the proposed study, we will explore if performing a memory task after a single session of Precuneus neuromodulation can be affected by selecting the point of the nine-point grid with the maximum signal propagation or the one with the lowest value. The selection of the two points of the nine-point grid will be at the subject level, so each patient will be behaviourally tested, choosing their point of maximum and minimum propagation value. Patients will do four experimental sessions. The first two will consist of an MRI acquisition, and the second will map the Precuneus with TMS-EEG (see Table 3). Then, once the coordinates of the interested points (the maximum and the minimum) are detected, patients will do two behavioral sessions. These two sessions will be counterbalanced in order and will be done a week apart. The stimulation will be a costimulation of "intermittent theta burst stimulation (iTBS) and transcranial alternate current stimulation (tACS) delivered in the gamma band (γtACS) based on previous studies" (Guerra et al., 2018; Maiella et al., 2022).

<table>
<tr><th colspan="5">Experimental Design</th></tr>
<tr><td>1st Session</td><td>2nd Session</td><td>3rd Session</td><td rowspan="3">One-week washout</td><td>4rd Session</td></tr>
<tr><td>MRI Acquisition</td><td>TMS-EEG</td><td rowspan="2">iTBS+tACS<br><br>Memory Task (FNAT)</td><td rowspan="2">iTBS+tACS<br><br>Memory Task (FNAT)</td></tr>
<tr><td>• Structural<br>• Resting fMRI<br>• DWI</td><td>• 9 grid points over Precuneus<br>• 64 EEG channel<br>• 60 pulses at adjusted TEP threshold<br>• ISI random 2-4 s</td></tr>
</table>

Table 3 - Experimental design for the proposed behavioral testing

The anode, which served as the active tACS electrode, will be positioned on the scalp beneath the iTBS coil, while the cathode will be placed on the right shoulder muscle. A Brainstim multifunctional system (E.M.S., Bologna s.r.l.) will deliver tACS through saline-soaked sponge electrodes measuring 7×5 cm2. The γtACS sinusoidal wave was configured at 70 Hz with a 1mA intensity, lasting for 190s. iTBS will be administered using a MagStim Rapid2 magnetic stimulator (Magstim Company, Whitland, Wales, UK) connected to a figure-of-eight coil (70 mm). This device produces a biphasic waveform pulse with a width of approximately 0.1 ms. The iTBS protocol consists of ten bursts, each containing three pulses at 50 Hz, delivered over 2 s. These bursts will be repeated every 10 s, with an 8 s interval between consecutive trains. Six hundred pulses will be administered over a 190 s period (Huang et al., 2005). We proposed using the Face Name Associate Task (FNAT) to test the memory. Immediately following the neuromodulation protocol, participants completed the FNAT, a cross-modal associative memory evaluation that requires individuals to match images of unknown faces with common first names and professions (Papp et al., 2014). The assessment comprised a learning stage followed by recall and recognition trials. During the learning phase, participants viewed 12 faces paired with names and occupations on a computer screen for 8 seconds each. They were instructed to vocalize the name and occupation to ensure focus on the items and to commit the face-name-occupation associations to memory. Immediately after learning, an instant cued recall phase occurred, where participants attempted to remember the name and occupation for each previously shown face, again displayed for 8 seconds. The delayed cued recall involved presenting the same faces and asking participants to recall each name and occupation. Lastly, in the recognition trial, participants had to identify the studied face from a distractor face of similar age and gender. For any unrecalled names or occupations, they were required to select the correct option from three choices, including a new name/occupation and one associated with a different face.

With the proposed study, we will test the combined neuromodulation protocol of iTBS and γtACS on a memory task in AD patients, evaluating the effect of the Precuneus stimulation point. We will test if choosing the stimulation Precuneus point with the higher signal propagation value may affect the efficacy of the neuromodulation protocol. The further results will shed more light on personalizing clinical and neurorehabilitative trials.

## 6.8 Implications, Insight, and Limitations

The reported results about the mapping of the Precuneus in AD patients come from a novel approach that has not previously been used. In this study, I proposed the integrated method of TMS, EEG, and MRI to obtain the spatio-temporal relation of Precuneus within the DMN "connectivity. The choice of proposing a methodologically integrated approach relies on the possibility of setting up an efficient tool for exploring connectivity in a comprehensive scenario" (Esposito et al., 2020). This approach has been very challenging, mainly because "no previous evidence could guide us in defining the best fitting of all the measurements at first" (Esposito et al., 2022). The last paragraphs have just reported the principal methodological limitations of our approach, but several are the points of strength. Firstly, "for each participant, we have been able to have the functional DMN, so it has been possible to find precisely the coordinates of the nodes to stimulate during the simultaneous TMS-EEG recordings. Moreover, these coordinates were used to monitor the coil's position during the registration to stimulate the same cortical node" with significant efficacy (Esposito et al., 2022). The functional and structural measurements were investigated individually, reporting a high constancy distribution among the sample. The high effectiveness "of the proposed method in measuring a stable response in time" is derived from the comparisons between the two TMS-EEG sessions (Esposito et al., 2022). The comparisons between the two neurophysiological recording outcomes support the method's efficacy in recording the same response in the same sample, with identical stimulation parameters, for all the stimulation conditions. This test-retest check is "evidence of the efficacy and replicability of the measurements of the novel proposed approach" (Esposito et al., 2022). The results support the idea that the MRI-guided TMS-EEG is a feasible tool for producing an efficient neurophysiological response to the functional organization of the DMN. "Moreover, from the integrated TMS, EEG, and MRI approach, it was possible to obtain" interesting information from the correlation between the source propagation and the neuroimaging indexes (Esposito et al., 2022). Correlations between source activation, functional resting state, and FA values produced informative outcomes about spreading activity dynamics. The results of the proposed new integrative approach will allow us to bring more evidence to the literature on methods for exploring brain functioning. "More evidence is needed to study the measurements obtained from the integrative approach and how they can replicate and/or integrate our results" (Esposito et al., 2022). The proposed integrative approach tested in the introduced study results to be a reliable and promising tool for exploring brain activity. In combining methods (TMS, EEG, MRI), we have to deal with the shortcomings of each single

method and the difficulties arising from the interactions. This work facilitates future research using the integration of TMS, EEG, MRI, and what has been difficult in this integration study, i.e., measuring functional connectivity with different methods and comparing it, using the cortical MRI coordinates with TMS-EEG, reconstructing structural pathways from functional cortical nodes, find the best statistical approach for investigating the correlation between the functional and structural data, define which measures to use in the correlation between the functional and structural data, is now getting more accessible. An important challenge for this study at present is the sample size. We will increase the cohort of patients to make the proposed outcomes more robust. Moreover, we plan to record a group of healthy controls matched per age to compare our results.

However, the results provide reliable evidence that combining different methods for exploring and detailing the Precuneus activity and connectivity is feasible to add more details of the dynamical integration for describing the information processing. More studies are needed on the spatio-temporal modifications occurring in the core regions at rest. “Future directions should explore more how, for instance, other structural connectivity indexes can replicate the comparison outcomes of this study, and analysis of higher-order, such as time-frequency, can describe the dynamical interaction” (Esposito et al., 2022).

To sum up, this study, even its intrinsic limitations, has reached an informative description of Precuneus activity from group to individual level comparison of the functional and structural information. Demonstrating its potential in describing the articulate integration between function and architecture, which lets the neural information processing.

## 6.9 Discussion

In this study, we have explored the neurophysiological characterization of the Precuneus region in AD patients through a multi-targeting Precuneus exploration. The proposed investigation has brought more evidence at both group and subject levels. The discussed results derive "from a methodologically integrated approach, with which we obtained a global view of the Precuneus connectivity within the DMN at a macroscopic level" (Esposito et al., 2022). The DMN nodes, congruent with the literature, have been extracted with a group ICA of the fMRI. The high congruency between the found DMN and the network found in literature provides strong evidence for the robust formation of functional DMN in the human brain (Damoiseaux et al., 2006; Marcus E Raichle, 2015; van den Heuvel, Mandl, Kahn, & Hulshoff Pol, 2009). In particular, we have focused on the Precuneus maximal activation coordinates, selected as the first point of the nine-point stimulation grid (see above). The outcome from the TMS-EEG recordings was used to explore if, at the group level, there was a difference in stimulating each point of the Precunes grid, testing the propagation of the signal between three brain regions involved in the DMN: the medial prefrontal area and the bilateral temporal lobes. After that, the source propagation for each patient was inspected. The neurophysiological recording has been evaluated at both sensor and source space, and their relation has been tested. Lastly, comparisons between the TMS-EEG and MRI signals have also been made. All these comparisons aimed to explore if mapping the activity propagation with TMS-EEG was a reliable method to characterize the spreading of neural reactivity and understand if it was feasible to study the individual characterization of Precuneus in AD. So that it is possible to find the best point for targeting the Precuneus activity for each participant, further comparisons with the functional and structural information may increase our knowledge of the resting dynamic in AD patients, obtaining a more comprehensive view of DMN connectivity.

The signal measured with TMS-EEG was analyzed in the source and time domain. The signal propagation has been investigated in the time window from 0 to 250 ms, evaluating the spreading of propagation in three ROIs: the medial frontal region and the bilateral temporal lobes. Instead, the neurophysiological responses (TEPs) have been analyzed in a restricted time window, from 11 to 100 ms, because evidence defines this interval as crucial for the signal spreading into the contralateral regions (Chung et al., 2015; Ilmoniemi et al., 1997; Parks et al., 2012). Firstly, it was assessed if the two TMS-EEG sessions differed so that non-parametric, cluster-based permutation statistics were conducted and corrected for multiple comparisons. A statistical comparison was made for both source and sensor space.

The analysis was performed on all electrodes in the time window from 0 to 250 and, for the source domain, and from 11 to 100 ms after the TMS pulse for the sensor space; all the comparisons did not reveal any differences in the two TMS-EEG sessions (all ps > 0.05, Figure 10 and 11). The present results suggest that the TEPs recorded with the same acquisition parameters in two longitudinal sessions are stable in time (Casarotto et al., 2010; Esposito et al., 2022). Proving how TEPs are a reliable neurophysiological measurement. Then, the difference in source propagation within the nine points of the Precuneus grid was assessed. The statistics reveal that the amount of signal propagation is lower in the upper row points of the grid (B, C), and it increases moving toward the bottom section of the grid. The points increase in terms of propagation and do not differ. Point A, the starting point for reconstructing the map over the Precuneus, results in a good point at the group level. This point is calculated based on the functional connectivity at the resting state. From this analysis, the evidence corroborates that point A has a high signal propagation level, which is also measured with TMS-EEG. However, at the same time, other points of the Precuneus map also reveal a good performance. In particular, it emerged that the posterior section of the grid presents points with a high signal propagation level, as the point extrapolated from the MRI, concerning the more anterior, which presents low propagation values. Moreover, inspecting the individual heatmap (Figure 14) makes it feasible to map the precuneus propagation and recognize the point with the highest and lowest propagation values for each AD patient. The described results demonstrate that it has been feasible with TMS-EEG to map the Precuneus activity and reactivity, recording a grid with nine different points. The nine-point grid recording demonstrated how TMS-EEG is sensible in measuring signals in a small area (9 $cm^2$). At the same time, it is also reliable and robust because the two sessions of TMS-EEG, recorded a month and a half apart, did not differ in measuring the brain activity in the same nine-point grid. So, the TMS-EEG mapping process seems reliable and sensitive in measuring the difference among all the grid points, allowing an informative distribution of Precuneus activity and reactivity at both group and individual levels in AD patients.

Furthermore, to evaluate the proposed approach more deeply, we ran a set of correlations to understand better the relation between all the neuroimaging methods and the different types of data information. In this way, we have found a link between the functional and structural connectivity within the DMN in AD patients. The first set of comparisons aimed to test whether there was a relation between the signal propagation and the amplitude of the TEP components. Significant positive correlations have emerged between the source propagation of points A, D, E, and I with the amplitude of the first three peaks, P30, N45, and P65. In

particular, the correlation for point A emerged between all the amplitude peaks and all the selected ROIs. So, the cortical reactivity is higher with increased signal propagation within the DMN. A significant positive correlation emerged for the other three significant points (D, E, and I) for the early TEPs component, P30, compared to different DMN ROIs. These reported correlations between the neurophysiological signals in two different domains demonstrate a positive correlation between the increase in signal propagation among the DMN in AD patients and their cortical reactivity. So, the more reactivity of the stimulated nodes, the more the signal is spread. Moreover, these correlations demonstrated that point A, which emerged from the MRI, presents several correlations between the DMN ROIs and all three amplitude peaks. Nevertheless, at the same time, other points have a strong positive correlation with cortical reactivity.

Instead, the second set of comparisons aimed to test the correlation between the signal spreading measured with TMS-EEG and the functional and structural indexes from MRI recordings. As reported above, two correlations emerged as significant, one for the functional activity of the hippocampus and one with the FA values of the Cingulum. The functional positive correlation emerged between the point with the minimum signal propagation of the right temporal lobe and the hippocampus activity. Instead, the second correlation is a negative correlation between the frontal source propagation of the point with the maximum activation and the FA values of the Cingulum. This preliminary correlation, run on a sample composed of ten patients, can lead us to understand that targeting the Precuneus activation has resonance in functional and structural connectivity within the DMN. Modification of this connectivity may shed more light on AD neurophysiology. In light of this, we support the DMN as a potential new target for neuromodulation therapy in Alzheimer's disease. Due to this, we have proposed a behavioral study (see above) for integrating the Precuneus mapping to identify, at the individual level, the points to test with a memory task and evaluate the effect of a neuromodulation protocol. We propose to study the points with the maximum activation level and, as a control, the ones with the minimum signal propagation level. With this experiment, it will be feasible to test if selecting a different point from the nine-point grid over the Precuneus impacts the DMN connectivity, moving from the neurophysiology to the behavioral field.

At this stage of development, it is relatively well established that the Precuneus plays a central role in resting-state functional and structural connectivity. We support the hypothesis that this dynamic integration involves an internal and external network relationship that efficiently sustains information processing.

## 6.10 Conclusion

In conclusion, this study provides “evidence of the efficacy of an integrative approach for” mapping the Precuneus activity and connectivity in a comprehensive scenario (Esposito et al., 2022). This experiment consists of a pioneering approach to exploring the neurophysiology in AD patients safely and non-invasively. Through the proposed nine-point grid, it has been feasible to characterize the Precuneus region of AD patients. The promising results open the main scenario of individualized neuromodulation protocol, intending to improve the benefits of TMS. Of course, this methodological approach can be applied to study other neurological and psychiatric diseases. So, the potentiality of the TMS as a tool for studying and treating brain activity and connectivity is improved. The methodologically integrated approach presents great potential in exploring the dynamically integrated temporal and spatial organization “of the default mode network and, in general, of the brain at rest in AD patients. The correlations between the neurophysiological data with the underlying pathways and functional connectivity have demonstrated the possibility of investigating connectivity dynamically” (Esposito et al., 2022). A significant advance highlighted here is that implementing a nine-point grid supports the neurophysiological characterization at the individual level. This would help the intervention phase by targeting the best stimulation site for the neuromodulation protocol. Improving the effect of non-invasive treatment for each patient will increase the chance of slowing down the progression of the disease.

Even if, until today, we have tested a sample of 15 patients, the outcomes appear clear and reliable. At the same time, we are working to make the sample bigger and our evidence more robust. Moreover, as described above, we are starting a new experimental procedure to test the efficacy in choosing the most valid point that emerged from the neurophysiological mapping in a behavioral field, intending to add more evidence on pursuing an individualized characterization and treatment. The proposed integrated approach represents a promising tool for the non-invasive investigation of the resting state dynamic in AD patients to reconstruct a deep and rich characterization of brain connectivity.

References


- Avena-Koenigsberger, A., Misic, B., & Sporns, O. (2017). Communication dynamics in complex brain networks. *Nature Reviews Neuroscience*, *19*, 17. Retrieved from https://doi.org/10.1038/nrn.2017.149
- Avena-Koenigsberger, A., Yan, X., Kolchinsky, A., van den Heuvel, M. P., Hagmann, P., & Sporns, O. (2019). A spectrum of routing strategies for brain networks. *PLOS Computational Biology*, *15*(3), e1006833. Retrieved from https://doi.org/10.1371/journal.pcbi.1006833
- Bäckman L, Small BJ, Fratiglioni L. (2001). Stability of the preclinical episodic memory deficit in Alzheimer's disease. Brain. Jan;124(Pt 1):96-102. doi: 10.1093/brain/124.1.96. PMID: 11133790.
- Bagattini, C., Mutanen, T. P., Fracassi, C., Manenti, R., Cotelli, M., Ilmoniemi, R. J., … Bortoletto, M. (2019). Predicting Alzheimer's disease severity by means of TMS–EEG coregistration. *Neurobiology of Aging*, *80*, 38–45. https://doi.org/https://doi.org/10.1016/j.neurobiolaging.2019.04.008
- Bandettini, P. A. (2012). Functional MRI: A confluence of fortunate circumstances. *NeuroImage*, *61*(2), A3–A11. https://doi.org/10.1016/j.neuroimage.2012.01.130
- Barker AT, Jalinous R, Freeston IL. (1985). Non-invasive magnetic stimulation of human motor cortex. Lancet. May 11;1(8437):1106–7. doi: 10.1016/s0140-6736(85)92413-4. PMID: 2860322.
- Basser PJ, Mattiello J, LeBihan D. (1994). Estimation of the effective self-diffusion tensor from the NMR spin echo. J Magn Reson B. Mar;103(3):247-54. doi: 10.1006/jmrb.1994.1037. PMID: 8019776.
- Bassett, Danielle S., & Sporns, O. (2017). Network neuroscience. *Nature Neuroscience*, *20*(3), 353–364. https://doi.org/10.1038/nn.4502
- Bassett, D. S., & Bullmore, E. (2006). Small-World Brain Networks. *The Neuroscientist*, *12*(6), 512–523. https://doi.org/10.1177/1073858406293182
- Bonato, C., Miniussi, C., & Rossini, P. M. (2006). Transcranial magnetic stimulation and cortical evoked potentials: A TMS/EEG co-registration study. *Clinical Neurophysiology*, *117*(8), 1699–1707. https://doi.org/10.1016/j.clinph.2006.05.006
- Borgatti, S. P., Mehra, A., Brass, D. J., & Labianca, G. (2009). Network analysis in the social sciences. *Science*, *323*(5916), 892–895. https://doi.org/10.1126/science.1165821
- Bortoletto, M., Veniero, D., Thut, G., & Miniussi, C. (2015). The contribution of TMS-EEG coregistration in the exploration of the human cortical connectome. *Neuroscience and Biobehavioral Reviews*, *49*, 114–124. https://doi.org/10.1016/j.neubiorev.2014.12.014
- Buckner, R. L., Andrews-Hanna, J. R., & Schacter, D. L. (2008). The Brain's Default Network. *Annals of the New York Academy of Sciences*, *1124*(1), 1–38. https://doi.org/10.1196/annals.1440.011

- Buckner, R. L., Snyder, A. Z., Shannon, B. J., LaRossa, G., Sachs, R., Fotenos, A. F., … Mintun, M. A. (2005). Molecular, structural, and functional characterization of Alzheimer's disease: evidence for a relationship between default activity, amyloid, and memory. *The Journal of Neuroscience : The Official Journal of the Society for Neuroscience*, *25*(34), 7709–7717. https://doi.org/10.1523/JNEUROSCI.2177-05.2005
- Bullmore, E., & Sporns, O. (2009). Complex brain networks: Graph theoretical analysis of structural and functional systems. *Nature Reviews Neuroscience*, *10*(3), 186–198. https://doi.org/10.1038/nrn2575
- Buzsáki G and Draguhn A. (2004). Neuronal oscillations in cortical networks. Science. Jun 25;304(5679):1926-9. doi: 10.1126/science.1099745. PMID: 15218136.
- Casarotto, S., Romero Lauro, L. J., Bellina, V., Casali, A. G., Rosanova, M., Pigorini, A., … Massimini, M. (2010). EEG Responses to TMS Are Sensitive to Changes in the Perturbation Parameters and Repeatable over Time. *PLOS ONE*, *5*(4), e10281. Retrieved from https://doi.org/10.1371/journal.pone.0010281
- Castellanos, F. X., Di Martino, A., Craddock, R. C., Mehta, A. D., & Milham, M. P. (2013). Clinical applications of the functional connectome. *NeuroImage*, *80*, 527–540. https://doi.org/10.1016/j.neuroimage.2013.04.083
- Casula EP, Pellicciari MC, Bonnì S, Borghi I, Maiella M, Assogna M, Minei M, Motta C, D'Acunto A, Porrazzini F, Pezzopane V, Mencarelli L, Roncaioli A, Rocchi L, Spampinato DA, Caltagirone C, Santarnecchi E, Martorana A, Koch G. (2022). Decreased Frontal Gamma Activity in Alzheimer Disease Patients. Ann Neurol. Sep;92(3):464-475. doi: 10.1002/ana.26444. Epub 2022 Jul 7. PMID: 35713198; PMCID: PMC9543336.
- Chen CK, Wu YT, Chang YC. (2017). Association between chronic periodontitis and the risk of Alzheimer's disease: a retrospective, population-based, matched-cohort study. Alzheimers Res Ther. Aug 8;9(1):56. doi: 10.1186/s13195-017-0282-6. PMID: 28784164; PMCID: PMC5547465.
- Chung, S. W., Rogasch, N. C., Hoy, K. E., & Fitzgerald, P. B. (2015). Measuring brain stimulation induced changes in cortical properties using TMS-EEG. *Brain stimulation*, *8*(6), 1010-1020.
- Cohen, M. X. (2017). Where does EEG come from and what does it mean? *Trends in Neurosciences*, *40*(4), 208–218.
- Colombo, M. A., Napolitani, M., Boly, M., Gosseries, O., Casarotto, S., Rosanova, M., … Sarasso, S. (2019). The spectral exponent of the resting EEG indexes the presence of consciousness during unresponsiveness induced by propofol, xenon, and ketamine. *NeuroImage*, *189*, 631–644. https://doi.org/https://doi.org/10.1016/j.neuroimage.2019.01.024
- Conde, V., Tomasevic, L., Akopian, I., Stanek, K., Saturnino, G. B., Thielscher, A., … Siebner, H. R. (2019). The non-transcranial TMS-evoked potential is an inherent source of ambiguity in

TMS-EEG studies. *NeuroImage*, *185*, 300–312. https://doi.org/https://doi.org/10.1016/j.neuroimage.2018.10.052

- Damoiseaux, J. S., Rombouts, S. A. R. B., Barkhof, F., Scheltens, P., Stam, C. J., Smith, S. M., & Beckmann, C. F. (2006). Consistent resting-state networks across healthy subjects. *Proceedings of the National Academy of Sciences of the United States of America*, *103*(37), 13848–13853. https://doi.org/10.1073/pnas.0601417103
- Day, B. L., Rothwell, J. C., Thompson, P. D., Dick, J. P. R., Cowan, J. M. A., Berardelli, A., & Marsden, C. D. (1987). Motor cortex stimulation in intact man: 2. Multiple descending volleys. *Brain*, *110*(5), 1191-1209.
- Dennis EL, Thompson PM. (2014). Functional brain connectivity using fMRI in aging and Alzheimer's disease. Neuropsychol Rev. 2014 Mar;24(1):49-62. doi: 10.1007/s11065-014-9249-6. Epub Feb 23. PMID: 24562737; PMCID: PMC4109887.
- Deriche, R. (2016). Computational brain connectivity mapping: A core health and scientific challenge. *Medical Image Analysis*, *33*, 122–126. https://doi.org/https://doi.org/10.1016/j.media.2016.06.003
- Deslauriers-Gauthier, S., Lina, J.-M., Butler, R., Whittingstall, K., Gilbert, G., Bernier, P.-M., … Descoteaux, M. (2019). White matter information flow mapping from diffusion MRI and EEG. *NeuroImage*, *201*, 116017. https://doi.org/https://doi.org/10.1016/j.neuroimage.2019.11601
- Di Lazzaro V, Oliviero A, Profice P, Insola A, Mazzone P, Tonali P, Rothwell JC. (1999). Direct demonstration of interhemispheric inhibition of the human motor cortex produced by transcranial magnetic stimulation. Exp Brain Res. Feb;124(4):520-4. doi: 10.1007/s002210050648. PMID: 10090664.
- Di Lazzaro V, Oliviero A, Profice P, Saturno E, Pilato F, Insola A, Mazzone P, Tonali P, Rothwell JC. (1998). Comparison of descending volleys evoked by transcranial magnetic and electric stimulation in conscious humans. Electroencephalogr Clin Neurophysiol. Oct;109(5):397-401. doi: 10.1016/s0924-980x(98)00038-1. PMID: 9851296.
- Dillen, K. N. H., Jacobs, H. I. L., Kukolja, J., Richter, N., von Reutern, B., Onur, O. A., … Fink, G. R. (2017). Functional Disintegration of the Default Mode Network in Prodromal Alzheimer's Disease. *Journal of Alzheimer's Disease : JAD*, *59*(1), 169–187. https://doi.org/10.3233/JAD-161120
- Ding, Y., Sohn, J. H., Kawczynski, M. G., Trivedi, H., Harnish, R., Jenkins, N. W., Lituiev, D., Copeland, T. P., Aboian, M. S., Mari Aparici, C., Behr, S. C., Flavell, R. R., Huang, S. Y., Zalocusky, K. A., Nardo, L., Seo, Y., Hawkins, R. A., Hernandez Pampaloni, M., Hadley, D., & Franc, B. L. (2019). A Deep Learning Model to Predict a Diagnosis of Alzheimer Disease by Using $^{18}$F-FDG PET of the Brain. *Radiology*, *290*(2), 456–464. https://doi.org/10.1148/radiol.2018180958
- Dubois, B., Hampel, H., Feldman, H. H., Scheltens, P., Aisen, P., Andrieu, S., Bakardjian, H.,

Benali, H., Bertram, L., Blennow, K., Broich, K., Cavedo, E., Crutch, S., Dartigues, J. F., Duyckaerts, C., Epelbaum, S., Frisoni, G. B., Gauthier, S., Genthon, R., Gouw, A. A., … (2016). Proceedings of the Meeting of the International Working Group (IWG) and the American Alzheimer's Association on "The Preclinical State of AD"; July 23, 2015; Washington DC, USA . Preclinical Alzheimer's disease: Definition, natural history, and diagnostic criteria. *Alzheimer's & dementia : the journal of the Alzheimer's Association*, *12*(3), 292–323. https://doi.org/10.1016/j.jalz.2016.02.002

- Esposito R, Bortoletto M, Miniussi C. (2020). Integrating TMS, EEG, and MRI as an Approach for Studying Brain Connectivity. Neuroscientist. Oct-Dec;26(5-6):471-486. doi: 10.1177/1073858420916452. Epub 2020 May 9. PMID: 32389094.
- Esposito R, Bortoletto M, Zacà D, Avesani P, Miniussi C. (2022). An integrated TMS-EEG and MRI approach to explore the interregional connectivity of the default mode network. Brain Struct Funct. Apr;227(3):1133-1144. doi: 10.1007/s00429-022-02453-6. Epub 2022 Feb 4. PMID: 35119502; PMCID: PMC8930884.
- Farzan, F., Barr, M. S., Levinson, A. J., Chen, R., Wong, W., Fitzgerald, P. B., & Daskalakis, Z. J. (2010). Reliability of Long-Interval Cortical Inhibition in Healthy Human Subjects: A TMS–EEG Study. *Journal of Neurophysiology*, *104*(3), 1339–1346. https://doi.org/10.1152/jn.00279.2010
- Friston KJ. (2011). Functional and effective connectivity: a review. Brain Connect. 1(1):13-36. doi: 10.1089/brain.2011.0008. PMID: 22432952.
- Friston, K. J., Frith, C. D., Liddle, P. F., & Frackowiak, R. S. J. (1993). Functional Connectivity: The Principal-Component Analysis of Large (PET) Data Sets. *Journal of Cerebral Blood Flow & Metabolism*, *13*(1), 5–14. https://doi.org/10.1038/jcbfm.1993.4
- Gili, T., Cercignani, M., Serra, L., Perri, R., Giove, F., Maraviglia, B., … Bozzali, M. (2011). Regional brain atrophy and functional disconnection across Alzheimer's disease evolution. *Journal of Neurology, Neurosurgery &Amp; Psychiatry*, *82*(1), 58 LP – 66. https://doi.org/10.1136/jnnp.2009.199935
- Guerra, A., Bologna, M., Paparella, G., Suppa, A., Colella, D., Di Lazzaro, V., Brown, P., & Berardelli, A. (2018). Effects of Transcranial Alternating Current Stimulation on Repetitive Finger Movements in Healthy Humans. *Neural plasticity*, *2018*, 4593095. https://doi.org/10.1155/2018/4593095
- Hernandez-Pavon, J. C., Veniero, D., Bergmann, T. O., Belardinelli, P., Bortoletto, M., Casarotto, S., Casula, E. P., Farzan, F., Fecchio, M., Julkunen, P., Kallioniemi, E., Lioumis, P., Metsomaa, J., Miniussi, C., Mutanen, T. P., Rocchi, L., Rogasch, N. C., Shafi, M. M., Siebner, H. R., Thut, G., … Ilmoniemi, R. J. (2023). TMS combined with EEG: Recommendations and open issues for data collection and analysis. *Brain stimulation*, *16*(2), 567–593. https://doi.org/10.1016/j.brs.2023.02.009
- Hill, A. T., Rogasch, N. C., Fitzgerald, P. B., & Hoy, K. E. (2016). TMS-EEG: A window into

the neurophysiological effects of transcranial electrical stimulation in non-motor brain regions. *Neuroscience & Biobehavioral Reviews*, *64*, 175–184. https://doi.org/https://doi.org/10.1016/j.neubiorev.2016.03.006

- Horvath, A., Szucs, A., Csukly, G., Sakovics, A., Stefanics, G., & Kamondi, A. (2018). EEG and ERP biomarkers of Alzheimer's disease: a critical review. *Frontiers in bioscience (Landmark edition)*, *23*(2), 183–220. https://doi.org/10.2741/4587
- Huang, Y. Z., Edwards, M. J., Rounis, E., Bhatia, K. P., & Rothwell, J. C. (2005). Theta burst stimulation of the human motor cortex. *Neuron*, *45*(2), 201–206. https://doi.org/10.1016/j.neuron.2004.12.033
- Hui, J., Tremblay, S., & Daskalakis, Z. J. (2019). The Current and Future Potential of Transcranial Magnetic Stimulation With Electroencephalography in Psychiatry. *Clinical Pharmacology & Therapeutics*, *0*(0). https://doi.org/10.1002/cpt.1541
- Ilmoniemi, R. J., Virtanen, J., Ruohonen, J., Karhu, J., Aronen, H. J., Näätänen, R., & Katila, T. (1997). Neuronal responses to magnetic stimulation reveal cortical reactivity and connectivity. *NeuroReport*, *8*(16), 3537–3540. https://doi.org/10.1097/00001756-199711100-00024
- Kerwin, L. J., Keller, C. J., Wu, W., Narayan, M., & Etkin, A. (2018). Test-retest reliability of transcranial magnetic stimulation EEG evoked potentials. *Brain Stimulation: Basic, Translational, and Clinical Research in Neuromodulation*, *11*(3), 536–544. https://doi.org/10.1016/j.brs.2017.12.010
- Kobayashi M, Pascual-Leone A. (2003). Transcranial magnetic stimulation in neurology. Lancet Neurol. Mar;2(3):145-56. doi: 10.1016/s1474-4422(03)00321-1. PMID: 12849236.
- Koch G, Casula EP, Bonnì S, Borghi I, Assogna M, Minei M, Pellicciari MC, Motta C, D'Acunto A, Porrazzini F, Maiella M, Ferrari C, Caltagirone C, Santarnecchi E, Bozzali M, Martorana A. (2022). Precuneus magnetic stimulation for Alzheimer's disease: a randomized, sham-controlled trial. Brain. Nov 21;145(11):3776-3786. doi: 10.1093/brain/awac285. PMID: 36281767; PMCID: PMC9679166.
- Koch, G. (2020). Transcranial Magnetic Stimulation in Dementia: From Pathophysiology to Treatment. *Non Invasive Brain Stimulation in Psychiatry and Clinical Neurosciences*, 161-173.
- Koch, G., Bonnì, S., Pellicciari, M. C., Casula, E. P., Mancini, M., Esposito, R., … Bozzali, M. (2018). Transcranial magnetic stimulation of the precuneus enhances memory and neural activity in prodromal Alzheimer's disease. *NeuroImage*, *169*, 302–311. https://doi.org/https://doi.org/10.1016/j.neuroimage.2017.12.048
- Koch, G., Martorana, A., & Caltagirone, C. (2019). Transcranial magnetic stimulation: Emerging biomarkers and novel therapeutics in Alzheimer's disease. *Neuroscience Letters*, 134355. https://doi.org/https://doi.org/10.1016/j.neulet.2019.134355
- Komssi, S., Aronen, H. J., Huttunen, J., Kesäniemi, M., Soinne, L., Nikouline, V. V, … Ilmoniemi, R. J. (2002). Ipsi- and contralateral EEG reactions to transcranial magnetic

stimulation. *Clinical Neurophysiology*, *113*(2), 175–184. https://doi.org/https://doi.org/10.1016/S1388-2457(01)00721-0

- Lerch, J. P., van der Kouwe, A. J. W., Raznahan, A., Paus, T., Johansen-Berg, H., Miller, K. L., … Sotiropoulos, S. N. (2017). Studying neuroanatomy using MRI. *Nature Neuroscience*, *20*(3), 314–326. https://doi.org/10.1038/nn.4501
- Lioumis, P., Kičić, D., Savolainen, P., Mäkelä, J. P., & Kähkönen, S. (2009). Reproducibility of TMS—Evoked EEG responses. *Human Brain Mapping*, *30*(4), 1387–1396. https://doi.org/10.1002/hbm.20608
- Luck, S. J. (2014). *An introduction to the event-related potential technique*. MIT press.
- Lundstrom BN, Ingvar M, Petersson KM. (2005) The role of precuneus and left inferior frontal cortex during source memory episodic retrieval. Neuroimage. Oct 1;27(4):824-34. doi: 10.1016/j.neuroimage.2005.05.008. PMID: 15982902.
- Maiella, M., Casula, E. P., Borghi, I., Assogna, M., D'Acunto, A., Pezzopane, V., ... & Koch, G. (2022). Simultaneous transcranial electrical and magnetic stimulation boost gamma oscillations in the dorsolateral prefrontal cortex. *Scientific Reports*, *12*(1), 19391.
- Maiella, M., Mencarelli, L., Casula, E. P., Borghi, I., Assogna, M., di Lorenzo, F., ... & Koch, G. (2024). Breakdown of TMS evoked EEG signal propagation within the default mode network in Alzheimer's disease. *Clinical Neurophysiology*, *167*, 177-188.
- Marchitelli, R., Minati, L., Marizzoni, M., Bosch, B., Bartres-Faz, D., Muller, B. W., … Jovicich, J. (2016). Test-retest reliability of the default mode network in a multi-centric fMRI study of healthy elderly: Effects of data-driven physiological noise correction techniques. *Human Brain Mapping*, *37*(6), 2114–2132. https://doi.org/10.1002/hbm.23157
- Mayeux R, Stern Y. (2012). Epidemiology of Alzheimer disease. Cold Spring Harb Perspect Med. Aug 1;2(8):a006239. doi: 10.1101/cshperspect.a006239. PMID: 22908189; PMCID: PMC3405821.
- Mencarelli, L., Monti, L., Romanella, S., Neri, F., Koch, G., Salvador, R., Ruffini, G., Sprugnoli, G., Rossi, S., & Santarnecchi, E. (2022). Local and Distributed fMRI Changes Induced by 40 Hz Gamma tACS of the Bilateral Dorsolateral Prefrontal Cortex: A Pilot Study. *Neural plasticity*, *2022*, 6197505. https://doi.org/10.1155/2022/6197505
- Mencarelli, L., Torso, M., Borghi, I., Assogna, M., Pezzopane, V., Bonnì, S., Di Lorenzo, F., Santarnecchi, E., Giove, F., Martorana, A., Bozzali, M., Ridgway, G. R., Chance, S. A., & Koch, G. (2024). Macro and micro structural preservation of grey matter integrity after 24 weeks of rTMS in Alzheimer's disease patients: a pilot study. *Alzheimer's research & therapy*, *16*(1), 152. https://doi.org/10.1186/s13195-024-01501-z
- Mevel K, Chételat G, Eustache F, Desgranges B. (2011). The default mode network in healthy aging and Alzheimer's disease. Int J Alzheimers Dis. 2011;2011:535816. doi: 10.4061/2011/535816. Epub Jun 14. PMID: 21760988; PMCID: PMC3132539.

- Menon, V., & Uddin, L. Q. (2010). Saliency, switching, attention and control: a network model of insula function. *Brain structure & function*, *214*(5-6), 655–667. https://doi.org/10.1007/s00429-010-0262-0
- Momi, D., Neri, F., Coiro, G., Smeralda, C., Veniero, D., Sprugnoli, G., ... & Santarnecchi, E. (2020). Cognitive enhancement via network-targeted cortico-cortical associative brain stimulation. *Cerebral Cortex*, *30*(3), 1516-1527.
- Morris JS, Frith CD, Perrett DI, Rowland D, Young AW, Calder AJ, Dolan RJ. (1996). A differential neural response in the human amygdala to fearful and happy facial expressions. Nature. Oct 31;383(6603):812-5. doi: 10.1038/383812a0. PMID: 8893004.
- Nakamura H, Kitagawa H, Kawaguchi Y, Tsuji H. (1996). Direct and indirect activation of human corticospinal neurons by transcranial magnetic and electrical stimulation. Neurosci Lett. May 24;210(1):45-8. doi: 10.1016/0304-3940(96)12659-8. PMID: 8762188.
- Nekkalapu, H. (2024). The Prevalence of Alzheimer's Disease and Hospital Readmissions Rates: A Retrospective Study.
- Nikouline, V., Ruohonen, J., & Ilmoniemi, R. J. (1999). The role of the coil click in TMS assessed with simultaneous EEG. *Clinical Neurophysiology*, *110*(8), 1325–1328. https://doi.org/https://doi.org/10.1016/S1388-2457(99)00070-X
- Ning, L., Makris, N., Camprodon, J. A., & Rathi, Y. (2019). Limits and reproducibility of resting-state functional MRI definition of DLPFC targets for neuromodulation. *Brain Stimulation: Basic, Translational, and Clinical Research in Neuromodulation*, *12*(1), 129–138. https://doi.org/10.1016/j.brs.2018.10.004
- Olivetti, E., Sharmin, N., & Avesani, P. (2016). Alignment of tractograms as graph matching. *Frontiers in Neuroscience*, *10*(DEC), 1–12. https://doi.org/10.3389/fnins.2016.00554
- Ongur, D., & Price, J. L. (2000). The organization of networks within the orbital and medial prefrontal cortex of rats, monkeys and humans. *Cerebral Cortex (New York, N.Y. : 1991)*, *10*(3), 206–219. https://doi.org/10.1093/cercor/10.3.206
- Oostenveld, R., Fries, P., Maris, E., & Schoffelen, J.-M. (2011). FieldTrip: Open source software for advanced analysis of MEG, EEG, and invasive electrophysiological data. *Computational Intelligence and Neuroscience*, *2011*, 156869. https://doi.org/10.1155/2011/156869
- Papp KV, Amariglio RE, Dekhtyar M, Roy K, Wigman S, Bamfo R, Sherman J, Sperling RA, Rentz DM. (2014). Development of a Psychometrically Equivalent Short Form of the Face–Name Associative Memory Exam for use Along the Early Alzheimer's Disease Trajectory. The Clinical Neuropsychologist 28:771–785. doi:10.1080/13854046.2014.91135
- Parks, N. A., Maclin, E. L., Low, K. A., Beck, D. M., Fabiani, M., & Gratton, G. (2012). Examining cortical dynamics and connectivity with simultaneous single-pulse transcranial magnetic stimulation and fast optical imaging. *NeuroImage*, *59*(3), 2504–2510. https://doi.org/10.1016/j.neuroimage.2011.08.097

- Pellicciari, M. C., Brignani, D., & Miniussi, C. (2013). Excitability modulation of the motor system induced by transcranial direct current stimulation: A multimodal approach. *NeuroImage*, *83*, 569–580. https://doi.org/https://doi.org/10.1016/j.neuroimage.2013.06.076
- Pellicciari, M. C., Veniero, D., & Miniussi, C. (2017). Characterizing the Cortical Oscillatory Response to TMS Pulse. *Frontiers in Cellular Neuroscience*, *11*(February), 1–5. https://doi.org/10.3389/fncel.2017.00038
- Petersen SE, Sporns O. (2015). Brain Networks and Cognitive Architectures. Neuron. Oct 7;88(1):207-19. doi: 10.1016/j.neuron.2015.09.027. PMID: 26447582; PMCID: PMC4598639.
- Porro-Muñoz, D., Olivetti, E., Sharmin, N., Nguyen, T. B., Garyfallidis, E., & Avesani, P. (2015). Tractome: a visual data mining tool for brain connectivity analysis. *Data Mining and Knowledge Discovery*, *29*(5), 1258–1279.
- Price, J. L. (2007). Definition of the orbital cortex in relation to specific connections with limbic and visceral structures and other cortical regions. *Annals of the New York Academy of Sciences*, *1121*, 54–71. https://doi.org/10.1196/annals.1401.008
- Ragazzoni, A., Cincotta, M., Giovannelli, F., Cruse, D., Young, G. B., Miniussi, C., & Rossi, S. (2017). Clinical neurophysiology of prolonged disorders of consciousness: From diagnostic stimulation to therapeutic neuromodulation. *Clinical Neurophysiology*, *128*(9), 1629–1646. https://doi.org/https://doi.org/10.1016/j.clinph.2017.06.037
- Raichle ME. (2015). The brain's default mode network. Annu Rev Neurosci. Jul 8;38:433-47. doi: 10.1146/annurev-neuro-071013-014030. Epub 2015 May 4. PMID: 25938726.
- Raichle ME. (2011). The restless brain. Brain Connect.1(1):3-12. doi: 10.1089/brain.2011.0019. PMID: 22432951; PMCID: PMC3621343.
- Raichle ME. (2010). Two views of brain function. Trends Cogn Sci. Apr;14(4):180-90. doi: 10.1016/j.tics.2010.01.008. Epub 2010 Mar 4. PMID: 20206576.
- Raichle, M E, MacLeod, A. M., Snyder, A. Z., Powers, W. J., Gusnard, D. A., & Shulman, G. L. (2001). A default mode of brain function. *Proceedings of the National Academy of Sciences of the United States of America*, *98*(2), 676–682. https://doi.org/10.1073/pnas.98.2.676
- Raichle, Marcus E. (2015). The Brain's Default Mode Network. *Annual Review of Neuroscience*, *38*(1), 433–447. https://doi.org/10.1146/annurev-neuro-071013-014030
- Reddy PH, Manczak M, Mao P, Calkins MJ, Reddy AP, Shirendeb U. (2010). Amyloid-beta and mitochondria in aging and Alzheimer's disease: implications for synaptic damage and cognitive decline. J Alzheimers Dis. ;20 Suppl 2(Suppl 2):S499-512. doi: 10.3233/JAD-2010-100504. PMID: 20413847; PMCID: PMC3059092.
- Rogasch NC, Sullivan C, Thomson RH, Rose NS, Bailey NW, Fitzgerald PB, Farzan F, Hernandez-Pavon JC. (2017). Analysing concurrent transcranial magnetic stimulation and electroencephalographic data: A review and introduction to the open-source TESA software. Neuroimage. Feb 15;147:934-951. doi: 10.1016/j.neuroimage.2016.10.031. Epub 2016 Oct 20.

PMID: 27771347.

- Rogasch, N. C., & Fitzgerald, P. B. (2013). Assessing cortical network properties using TMS-EEG. *Human Brain Mapping*, *34*(7), 1652–1669. https://doi.org/10.1002/hbm.22016
- Rosanova, M., Mariotti, M., Bellina, V., Casali, A., Resta, F., & Massimini, M. (2009). Natural Frequencies of Human Corticothalamic Circuits. *Journal of Neuroscience*, *29*(24), 7679–7685. https://doi.org/10.1523/jneurosci.0445-09.2009
- Rossi, S., Hallett, M., Rossini, P. M., & Pascual-Leone, A. (2011, August). Screening questionnaire before TMS: an update. *Clinical Neurophysiology : Official Journal of the International Federation of Clinical Neurophysiology*. Netherlands. https://doi.org/10.1016/j.clinph.2010.12.037
- Rossini, P. M., Burke, D., Chen, R., Cohen, L. G., Daskalakis, Z., Di Iorio, R., … Ziemann, U. (2015). Non-invasive electrical and magnetic stimulation of the brain, spinal cord, roots and peripheral nerves: Basic principles and procedures for routine clinical and research application. An updated report from an I.F.C.N. Committee. *Clinical Neurophysiology : Official Journal of the International Federation of Clinical Neurophysiology*, *126*(6), 1071–1107. https://doi.org/10.1016/j.clinph.2015.02.001
- Rossini, P. M., Di Iorio, R., Bentivoglio, M., Bertini, G., Ferreri, F., Gerloff, C., … Hallett, M. (2019). Methods for analysis of brain connectivity: An IFCN-sponsored review. *Clinical Neurophysiology*, *130*(10), 1833–1858. https://doi.org/https://doi.org/10.1016/j.clinph.2019.06.006
- Sammet, S. (2016). Magnetic resonance safety. *Abdominal Radiology (New York)*, *41*(3), 444–451. https://doi.org/10.1007/s00261-016-0680-4
- Seghier, M. L., & Friston, K. J. (2013). Network discovery with large DCMs. *NeuroImage*, *68*, 181–191. https://doi.org/https://doi.org/10.1016/j.neuroimage.2012.12.005
- Seitz, R. J., Franz, M., & Azari, N. P. (2009). Value judgments and self-control of action: the role of the medial frontal cortex. *Brain Research Reviews*, *60*(2), 368–378. https://doi.org/10.1016/j.brainresrev.2009.02.003
- Shulman, G. L., Fiez, J. A., Corbetta, M., Buckner, R. L., Miezin, F. M., Raichle, M. E., & Petersen, S. E. (1997). Common Blood Flow Changes across Visual Tasks: II. Decreases in Cerebral Cortex. *Journal of Cognitive Neuroscience*, *9*(5), 648–663. https://doi.org/10.1162/jocn.1997.9.5.648
- Siebner, H. R., Bergmann, T. O., Bestmann, S., Massimini, M., Johansen-Berg, H., Mochizuki, H., … Rossini, P. M. (2009). Consensus paper: Combining transcranial stimulation with neuroimaging. *Brain Stimulation*, *2*(2), 58–80. https://doi.org/10.1016/j.brs.2008.11.002
- Sperling, R. A., Aisen, P. S., Beckett, L. A., Bennett, D. A., Craft, S., Fagan, A. M., Iwatsubo, T., Jack, C. R., Jr, Kaye, J., Montine, T. J., Park, D. C., Reiman, E. M., Rowe, C. C., Siemers, E., Stern, Y., Yaffe, K., Carrillo, M. C., Thies, B., Morrison-Bogorad, M., Wagster, M. V., …

Phelps, C. H. (2011). Toward defining the preclinical stages of Alzheimer's disease: recommendations from the National Institute on Aging-Alzheimer's Association workgroups on diagnostic guidelines for Alzheimer's disease. *Alzheimer's & dementia : the journal of the Alzheimer's Association*, *7*(3), 280–292. https://doi.org/10.1016/j.jalz.2011.03.003

- Sporns O, Tononi G, Kötter R. (2005). The human connectome: A structural description of the human brain. PLoS Comput Biol. Sep;1(4):e42. doi: 10.1371/journal.pcbi.0010042. PMID: 16201007; PMCID: PMC1239902.
- Sporns, O. (2011). The human connectome: A complex network. *Annals of the New York Academy of Sciences*, *1224*(1), 109–125. https://doi.org/10.1111/j.1749-6632.2010.05888.x
- Sporns, O. (2013). The human connectome: Origins and challenges. *NeuroImage*, *80*, 53–61. https://doi.org/10.1016/j.neuroimage.2013.03.023
- Sporns, O., & Betzel, R. F. (2016). *Modular Brain Networks*. *SSRN*. https://doi.org/10.1146/annurev-psych-122414-033634
- Stephan, K. E., Kasper, L., Brodersen, K. H., & Mathys, C. D. (2009). Functional and effective connectivity. *Klinische Neurophysiologie*, *40*(04), 222–232.
- Tadel, F., Baillet, S., Mosher, J. C., Pantazis, D., & Leahy, R. M. (2011). Brainstorm: a user-friendly application for MEG/EEG analysis. *Computational intelligence and neuroscience*, *2011*, 879716. https://doi.org/10.1155/2011/879716
- Tadić B, Andjelković M, Melnik R. (2019). Functional Geometry of Human Connectomes. Sci Rep. Aug 19;9(1):12060. doi: 10.1038/s41598-019-48568-5. PMID: 31427676; PMCID: PMC6700117.
- ter Braack, E. M., de Vos, C. C., & van Putten, M. J. A. M. (2015). Masking the Auditory Evoked Potential in TMS--EEG: A Comparison of Various Methods. *Brain Topography*, *28*(3), 520–528. https://doi.org/10.1007/s10548-013-0312-z
- Thut, G., & Miniussi, C. (2009). New insights into rhythmic brain activity from TMS-EEG studies. *Trends in Cognitive Sciences*, *13*(4), 182–189. https://doi.org/10.1016/j.tics.2009.01.004
- Thut, G., & Pascual-Leone, A. (2010). Editorial: Integrating TMS with EEG: How and what for? *Brain Topography*, *22*(4), 215–218. https://doi.org/10.1007/s10548-009-0128-z
- Thut, G., Bergmann, T. O., Fröhlich, F., Soekadar, S. R., Brittain, J. S., Valero-Cabré, A., … Herrmann, C. S. (2017). Guiding transcranial brain stimulation by EEG/MEG to interact with ongoing brain activity and associated functions: A position paper. *Clinical Neurophysiology*, *128*(5), 843–857. https://doi.org/10.1016/j.clinph.2017.01.003
- Tournier, J.-D., Calamante, F., & Connelly, A. (2007). Robust determination of the fibre orientation distribution in diffusion MRI: non-negativity constrained super-resolved spherical deconvolution. *Neuroimage*, *35*(4), 1459–1472.
- Ugurbil, K. (2016). What is feasible with imaging human brain function and connectivity using functional magnetic resonance imaging. *Philosophical Transactions of the Royal Society of*

*London. Series B, Biological Sciences*, *371*(1705). https://doi.org/10.1098/rstb.2015.0361

- Umeda, S. (2018). Functional Anatomy of Encoding/Retrieval Processing in the Medial Parietal Areas. *Brain and nerve = Shinkei kenkyu no shinpo*, *70*(7), 763–769. https://doi.org/10.11477/mf.1416201077
- van den Heuvel, M. P., Mandl, R. C. W., Kahn, R. S., & Hulshoff Pol, H. E. (2009). Functionally linked resting-state networks reflect the underlying structural connectivity architecture of the human brain. *Human Brain Mapping*, *30*(10), 3127–3141. https://doi.org/10.1002/hbm.20737
- Veldsman M. (2017). Brain Atrophy Estimated from Structural Magnetic Resonance Imaging as a Marker of Large-Scale Network-Based Neurodegeneration in Aging and Stroke. *Geriatrics (Basel, Switzerland)*, *2*(4), 34. https://doi.org/10.3390/geriatrics2040034
- Voineskos, A. N., Farzan, F., Barr, M. S., Lobaugh, N. J., Mulsant, B. H., Chen, R., … Daskalakis, Z. J. (2010). The Role of the Corpus Callosum in Transcranial Magnetic Stimulation Induced Interhemispheric Signal Propagation. *Biological Psychiatry*, *68*(9), 825–831. https://doi.org/10.1016/j.biopsych.2010.06.021
- Wagner AD, Shannon BJ, Kahn I, Buckner RL. (2005). Parietal lobe contributions to episodic memory retrieval. Trends Cogn Sci. Sep;9(9):445-53. doi: 10.1016/j.tics.2005.07.001. PMID: 16054861.
- Whitfield-Gabrieli, S., & Nieto-Castanon, A. (2012). Conn: a functional connectivity toolbox for correlated and anticorrelated brain networks. *Brain connectivity*, *2*(3), 125–141. https://doi.org/10.1089/brain.2012.0073
- Wu X, Li R, Fleisher AS, Reiman EM, Guan X, Zhang Y, Chen K, Yao L. (2011). Altered default mode network connectivity in Alzheimer's disease--a resting functional MRI and Bayesian network study. Hum Brain Mapp. Nov;32(11):1868-81. doi: 10.1002/hbm.21153. Epub 2011 Jan 21. PMID: 21259382; PMCID: PMC3208821.
- Xu, J., Yin, X., Ge, H., Han, Y., Pang, Z., Liu, B., Liu, S., & Friston, K. (2017). Heritability of the Effective Connectivity in the Resting-State Default Mode Network. *Cerebral cortex (New York, N.Y. : 1991)*, *27*(12), 5626–5634. https://doi.org/10.1093/cercor/bhw332
- Yeh, F. C., Wedeen, V. J., & Tseng, W. Y. I. (2010). Generalized ${q} $-sampling imaging. *IEEE transactions on medical imaging*, *29*(9), 1626-1635.
- Ziemann, U., & Siebner, H. R. (2015). Inter-subject and inter-session variability of plasticity induction by non-invasive brain stimulation: boon or bane? *Brain Stimulation: Basic, Translational, and Clinical Research in Neuromodulation*, *8*(3), 662–663.